the absence (open symbols) or presence (closed symbols) of 150 mM NaCl, indicating a sharp LCST-type phase transition. The LCST values were found to linearly increase with the increasing mol % of EtOx (n), from 38.7 °C (or 37.4 °C) at n = 0% to 67.3 °C (or 65.4 °C) at n = 75% for a 1.0 wt % polymer solution in the absence (or presence) of 150 mM NaCl (Figure 11b). Regardless of the *i*PrOx to EtOx ratio, an exceedingly clear sensitivity of the phase separation was observed in all cases, whereas no change in transmittance appeared in the case of a PEtOx homopolymer at the measured temperatures up to 90 °C (Table 1). It was also observed that the LCST values of the (co)polymer solutions in the presence of 150 mM NaCl, viz., near the physiological condition, slightly shifted to lower temperatures in all cases compared to that in the absence of NaCl. This result was in agreement with the well-known "salting-out" effect of NaCl.[23]

A notable point of these turbidity results is that observed transition was appreciably sharp and simply correlated with the ratio of both monomers in the copolymers even though they have the compositional gradient along the polymer strand. It may be reasonable to assume that the LCST property of such a gradient copolymer may become complicated due to a possible formation of micelle-like molecular association derived from a deviating amphiphilicity along the polymer chain. Nevertheless, the static light scattering (SLS) measurements of the solution with varying temperature provided no obvious sign of assembly formation, keeping the weak and constant scattering intensity up to the LCST (data not shown). Although we may not exclude the possibility of conformational change in a single strand of the gradient copolymers below LCST due to the deviating amphiphilicity in the strand, turbidity behavior follows a rather simple and practical rule to be correlated with the ratio of both monomers in the copolymers. Detailed solution behavior of these gradient copolymers should be an important topic for the further study to understand their actual molecular dynamics related to temperature change, yet the present study recalls the well-established oxazoline polymerization as a convenient procedure to obtain the copolymers with extremely narrow molecular weight distribution and finely tuned LCST.

Conclusions

This study developed the facile and precise synthetic route of thermosensitive POx gradient copolymers via the living cationic polymerization of 2-isopropyl-2-oxazoline (*i*PrOx) mixed with a specific composition of 2-ethyl-2-oxazoline (EtOx) as a hydrophilic comonomer. The oxazoline monomers (EtOx and *i*PrOx) had sufficiently different reactivity ratios of 1.78 and 0.79, respectively, leading to obtain the gradient copolymers with varying composition and very narrow molecular weight distribution. Turbidity measurements revealed that LCST of the gradient copolymers can be minutely modulated over a broad range of temperature from 38.7 to 67.3 °C simply by varying the molar ratio of EtOx to *i*PrOx. This approach of copolymerizing a variety of oxazoline monomers with different hydrophobic and hydrophilic balance, in a condition to attain living polymerization (mild temperature in acetonitrile), apparently lead to the systematic preparation of versatile end-functionalized polyoxazoline derivatives with finely tuned LCST, which have a promising feasibility particularly in biomedical applications as constructing thermosensitive bioconjugates and drug delivery systems.

Acknowledgment. This work was financially supported by Special Coordination Funds for Science and Technology from the Ministry of Education, Culture, Sports, Science and Technology of Japan (MEXT) as well as by the Core Research for Evolutional Science and Technology (CREST) from the Japan Science and Technology Agency (JST).

Supporting Information Available: Figures S1−S6 and Tables S1 and S2. This material is available free of charge via the Internet at http://pubs.acs.org.

References and Notes

(1) (a) Bergbreiter, D. E.; Osburn, P. L.; Wilson, A.; Sink, E. M. *J. Am. Chem. Soc.* **2000**, *122*, 9058. (b) Hamamoto, H.; Suzuki, Y.; Yamada, Y.; Tabata, H.; Takahashi, H.; Ikegami, S. *Angew. Chem., Int. Ed.* **2005**, *44*, 4536.

(2) (a) Uchiyama, S.; Kawai, N.; de Silva, A. P.; Iwai, K. *J. Am. Chem. Soc.* **2004**, *126*, 3032. (b) Hu, Z. B.; Chen, Y. Y.; Wang, C. J.; Zheng, Y. D.; Li, Y. *Nature (London)* **1998**, *393*, 149.

(3) (a) Kanazawa, H.; Yamamoto, K.; Matsushima, Y.; Takai, N.; Kikuchi, A.; Sakurai, Y.; Okano, T. *Anal. Chem.* **1996**, *68*, 100. (b) Kikuchi, A.; Okano, T. *Prog. Polym. Sci.* **2002**, *27*, 1165.

(4) (a) Stayton, P. S.; Shimoboji, T.; Long, C.; Chilkoti, A.; Chen, G.; Harris, J. M.; Hoffman, A. S. *Nature (London)* **1995**, *378*, 472. (b) Matsukata, M.; Aoki, T.; Sanui, K.; Ogata, N.; Kikuchi, A.; Sakurai, Y.; Okano, T. *Bioconjugate Chem.* **1996**, *7*, 96. (c) Ding, Z.; Chen, G.; Hoffman, A. S. *J. Biomed. Mater. Res.* **1998**, *39*, 498.

(5) (a) Yoshida, R.; Sakai, T.; Okano, T.; Sakurai, Y.; Bae, Y. H.; Kim, S. W. *J. Biomater. Sci., Polym. Ed.* **1991**, *3*, 155. (b) Cammas, S.; Suzuki, K.; Sone, Y.; Kakurai, Y.; Kataoka, K.; Okano, T. *J. Controlled Release* **1997**, *48*, 157. (c) Kono, K. *Adv. Drug. Deliv. Rev.* **2001**, *53*, 307.

(6) (a) Park, J. S.; Akiyama, Y.; Winnik, F. M.; Kataoka, K. *Macromolecules* **2004**, *37*, 6786. (b) Diab, C.; Akiyama, Y.; Kataoka, K.; Winnik, F. M. *Macromolecules* **2004**, *37*, 2556.

(7) (a) Kobayashi, S. *Prog. Polym. Sci.* **1990**, *15*, 751. (b) Aoi, K.; Okada, M. *Prog. Polym. Sci.* **1996**, *21*, 151. (c) Kobayashi, S.; Uyama, H. *J. Polym. Sci., Part A: Polym. Chem.* **2002**, *40*, 192.

(8) (a) Heskins, M.; Guillent, J. E.; James, E. J. *J. Macromol. Sci., Chem.* **1968**, *A2*, 1441. (b) Schild, H. G. *Prog. Polym. Sci.* **1992**, *17*, 163.

(9) (a) Woodle, M. C.; Engbers, C. M.; Zalipsky, S. *Bioconjugate Chem.* **1994**, *5*, 493. (b) Zalipsky, S.; Hansen, C. B.; Oaks, J. M.; Allen, T. M. *J. Pharm. Sci.* **1996**, *85*, 133.

(10) (a) Taylor, L. D.; Cerankowski, L. D. *J. Polym. Sci.* **1975**, *13*, 2551. (b) Feil, H.; Bae, Y. H.; Feijen, J.; Kim, S. W. *Macromolecules* **1993**, *26*, 2496.

(11) (a) Sugihara, S.; Kanaoka, S.; Aoshima, S. *Macromolecules* **2004**, *37*, 1711. (b) Ali, M. M.; Stöver, H. D. H. *Macromolecules* **2004**, *37*, 5219. (c) Mori, H.; Iwaya, H.; Nagai, A.; Endo, T. *Chem. Commun.* **2005**, *38*, 4872. (d) Lutz, J.; Hoth, A. *Macromolecules* **2006**, *39*, 893.

(12) (a) Kagiya, T.; Matsuda, T.; Nakato, M.; Hirata, R. *J. Macromol. Sci., Chem.* **1972**, *6*, 1631. (b) Cai, G.; Litt, M. *J. Polym. Sci., Part A: Polym. Chem.* **1992**, *30*, 649. (c) Hoogenboom, R.; Fijten, M. W. M.; Schubert, U. S. *J. Polym. Sci., Part A: Polym. Chem.* **2004**, *42*, 1830.

(13) (a) Pakula, T.; Matyjaszewski, K. *Macromol. Theory Simul.* **1996**, *5*, 987. (b) Matyjaszewski, K.; Ziegler, M. J.; Arehart, S. V.; Greszta, D.; Pakula, T. *J. Phys. Org. Chem.* **2000**, *13*, 775.

(14) Seeliger, W.; Aufderhaar, E.; Diepers, W.; Feinauer, R.; Nehring, R.; Their, W.; Hellmann, H. *Angew. Chem., Int. Ed. Engl.* **1966**, *5*, 875.

(15) Perrin, D. D.; Armarego, W. L. F.; Perrin, D. R. *Purification of Laboratory Chemicals*; Pergamon: Oxford, 1980.

(16) (a) Levy, A.; Litt, M. *J. Polym. Sci., Part A-1* **1968**, *6*, 1883. (b) Litt, M.; Levy, A.; Herz, J. *J. Macromol. Sci., Chem.* **1975**, *A9*, 703. (c) Warakomski, J. M.; Thill, B. P. *J. Polym. Sci., Part A* **1990**, *28*, 3551.

(17) (a) Liu, Q.; Konas, M.; Riffle, J. S. *Macromolecules* **1993**, *26*, 5572. (b) Chen, C. H.; Wilson, J.; Chen, W.; Davis, R. M.; Riffle, J. S. *Polymer* **1994**, *35*, 3587. (c) Kobayashi, S.; Masuda, E.; Shoda, S.; Shimano, Y. *Macromolecules* **1989**, *22*, 2878. (d) Wiesbrock, F.; Hoogenboom, R.; Leenen, M. A. M.; Meier, M. A. R.; Schubert, U. S. *Macromolecules* **2005**, *38*, 5025.

(18) Madruga, E. L. *Prog. Polym. Sci.* **2002**, *27*, 1879.

(19) (a) Saegusa, T.; Ikeda, H.; Fujii, H. *Macromolecules* **1973**, *6*, 315. (b) Saegusa, T.; Kobayashi, S.; Yamada, A. *Makromol. Chem.* **1976**, *177*, 2271. (c) Uyama, H.; Kobayashi, S. *Macromolecules* **1991**, *24*, 614.

(20) Hagipol, C. *Copolymerization-Toward a Systematic Approach*; Kluwer Academic: New York, 1999.

(21) (a) Montaudo, M. S. *Rapid Commun. Mass Spectrom.* **1999**, *13*, 639. (b) Montaudo, M. S. *Mass Spectrom. Rev.* **2002**, *21*, 108.

(22) Terrier, P.; Buchmann, W.; Cheguillaume, G.; Desmazières, B.; Tortajada, J. *Anal. Chem.* **2005**, *77*, 3292.

(23) Lin, P.; Pearce, E. M.; Kwei, T. K. *J. Polym. Sci., Part B: Polym. Phys.* **1988**, *26*, 603.

MA0605548

Mod Rheumatol (2006) 16:24–29
DOI 10.1007/s10165-005-0450-6

ORIGINAL ARTICLE

**Noriko Yoshimura · Hirofumi Kinoshita · Noriaki Hori
Taira Nishioka · Masahiko Ryujin · Yoshihiko Mantani
Mariko Miyake · Tatsuya Takeshita · Masao Ichinose
Munehito Yoshiida · Hiroyuki Oka · Hiroshi Kawaguchi
Kozo Nakamura · Cyrus Cooper**

Risk factors for knee osteoarthritis in Japanese men: a case-control study

Received: July 27, 2005 / Accepted: December 13, 2005

Abstract Risk of knee osteoarthritis (OA) was assessed in a population-based case-control study of Japanese men. The study covered three health districts in Wakayama and Osaka prefectures, Japan. Subjects were male individuals ≥45 years old diagnosed radiographically with knee OA, and who did not display any established causes of secondary OA. Controls selected randomly from the general population were individually matched to cases for age, sex, and residential district. Subjects were interviewed using structured questionnaires to determine medical history, physical activity, socio-economic factors, and occupation. Interviews were obtained from 37 cases and 37 controls. In univariate analysis, heaviest weight in the past and physical work such as factory, construction, agricultural, or fishery work as the principal occupation significantly raised the risk of male knee OA ($P < 0.05$). Odds ratios (OR) were determined using conditional logistic regression analysis mutually adjusted for potential risk factors using the results of univariate analysis. Heaviest weight in the past (OR 6.01, 95% confidence interval (CI) 1.18–30.5, $P < 0.05$), past knee injury (OR 6.25, 95% CI 1.13–34.5, $P < 0.05$), and physical work as the principal occupation (OR 6.20, 95% CI 1.40–27.5, $P < 0.05$) represented independent factors associated with knee OA after controlling for other risk factors. Physical work is associated with knee OA, demonstrating the influence of working activity on the development of OA. The present study suggests that risk factors for knee OA in men resemble those in women.

Key words Case control study · Heavy weight · Knee joint · Osteoarthritis (OA)· Physical work

N. Yoshimura (✉) · H. Oka
Department of Joint Disease Research, Graduate School of Medicine, The University of Tokyo, 7-3-1 Hongo, Bunkyo-ku, Tokyo 113-8655, Japan
Tel. +81-3-5800-9178; Fax +81-3-5800-9179
e-mail: yoshimuran-ort@h.u-tokyo.ac.jp

H. Kinoshita
Department of Orthopaedic Surgery, Wakayama Medical University Kihoku Hospital, Wakayama, Japan

N. Hori
Hori Hospital, Sennan, Japan

T. Nishioka
Nishioka Orthopaedic Hospital, Arita, Japan

M. Ryujin
Ryujin Clinic, Wakayama, Japan

Y. Mantani
Tamai Orthopaedic Hospital, Hannan, Japan

M. Miyake
Yamomoto Clinic, Shimotsu, Japan

T. Takeshita
Department of Public Health, Wakayama Medical University School of Medicine, Wakayama, Japan

M. Ichinose
Second Department of Internal Medicine, Wakayama Medical University School of Medicine, Wakayama, Japan

M. Yoshiida
Department of Orthopaedic Surgery, Wakayama Medical University School of Medicine, Wakayama, Japan

H. Kawaguchi · K. Nakamura
Department of Orthopaedic Surgery, Faculty of Medicine, The University of Tokyo, Tokyo, Japan

C. Cooper
MRC Epidemiology Resource Centre, University of Southampton, Southampton General Hospital, Southampton, UK

Introduction

Since osteoarthritis (OA) is a frequent cause of pain and disability in elderly individuals, the recent World Health Organization report on the global burden of disease indicated knee OA as an increasingly important cause of disability in both men and women, suggesting that strategies for preventing OA are urgently required.[1] In Japan, knee OA seems to represent a frequent cause of pain and disability, but few epidemiological studies have examined associated factors.

Several investigations regarding risk factors for hip and knee OA performed in Western populations have

suggested obesity, previous injury, polyarticular joint involvement, and occupational activities as important risk factors for the disorder.[2–8] However, few studies of risk factors for OA in Japanese populations have been performed. Our earlier case-control study of hip OA identified some variations in risk factors in Japan.[9] In the previous case-control study of hip OA, occupational lifting was identified as a risk factor and sedentary work as a protective factor for hip OA. In addition, obesity was not identified as a risk factor for Japanese hip OA. For contrast, an identical case-control study was performed for knee OA in women in a Japanese population.[10] In the female study, risk factors of obesity, previous knee injury, and period of total work were identified, and sedentary work as the initial occupation represented a preventive factor.[10] The results from these two investigations suggest various similarities and differences in risk factors between hip and knee OA in Japanese populations.

The present study sought to clarify risk factors for knee OA among men in Japan, by performing a survey identical to that used in the previous female knee OA study. Results for men were compared to those from the female study.[10] Risk factors were then compared between knee OA and hip OA to address differences in risk factors for constitutional and mechanical factors between OA at different sites. Finally, risk factors for knee and hip OA were compared to those identified in a British study[11,12] that used identical methods to the Japanese studies, to clarify differences in risk factors for OA between Japanese and Western populations.

Patients and methods

Methods of data collection in the present study were basically identical to those of the case-control studies for female knee OA and hip OA reported previously.[9,10] A brief summary is provided here. Cases were identified from the registration systems of the six hospitals participating in the study, which were located in three cities in Japan (Wakayama City and Arita City in Wakayama Prefecture, and Sennan City in Osaka Prefecture).

Cases comprised men ≥45 years old who suffered knee pain and walking difficulties, and who were first diagnosed by an orthopedic surgeon as displaying a tibiofemoral joint with radiographic grade of ≥3 on the Kellgren and Lawrence scale[13] within the year preceding the start of the study. Cases with a history of knee injury in the previous year, rheumatoid arthritis, or ankylosing spondylitis were excluded.

For each case, a single control was randomly selected from among men of the same age and district of residence on city registers of the local population, which are updated as residents move into or leave the city. Controls who had suffered knee OA were excluded from the study.

All eligible cases and controls were initially approached using a letter to determine willingness to participate in the study. After providing informed consent, cases and controls were interviewed by the same trained interviewer.

An identical questionnaire to that used in the British case-control study was used to ascertain risk factors of knee OA.[11,12] The questionnaire was translated and back-translated from Japanese to English. Subjects completed a structured questionnaire that requested details of medical history, socio-economic status and education, cigarette smoking and alcohol consumption, functional status, and lifetime history of leisure activities. Lifetime history of leisure activities included participation in sports such as soccer, swimming, tennis, cricket, and golf, in addition to frequency and duration of less physical activities, such as gardening. Information about eight types of occupational physical activity was requested, namely: standing; sitting; climbing stairs; kneeling; squatting; driving; walking; and heavy lifting. Information on these activities was obtained for the initial job, defined as the earliest job reported, and for the principal job, defined as the job at which the subject had worked longest. For each job, the questionnaire enquired whether work entailed lifting weights (≥10 kg, ≥25 kg, or ≥50 kg) more than once during an average working week. Information regarding use of transport, including frequency and duration of cycling and motorcycling was obtained. Information was also requested on the involvement of other joints, including hands, shoulders, and hips. Furthermore, questions were added about back pain and stiffness, which were not included in the British study. Once heaviest reported weight after 25 years old was obtained, height and weight of each subject was measured at the time of the interview.

After analysis to clarify risk for male knee OA, results were compared between men and published results for women.[10] Risk factors for knee OA and hip OA were also compared to address differences in constitutional and mechanical risk factors between OA at different sites. Finally, risk factors for knee and hip OA were compared to the findings of the British study, which used identical methods to the Japanese studies.

Data were calculated using McNemar's Chi-square test and conditional logistic regression tests for matched sets. Results were summarized as odds ratios (OR) with 95% confidence intervals (CI). Odds ratios were calculated for categories of exposure, and tests of trend were performed across these categories. Statistical analyses were performed using SPSS statistical software (SPSS, Chicago, IL, USA) and the STATA statistical package (STATA, College Station, TX, USA).

Results

A total of 40 men ≥45 years old fulfilled the entry criteria for the study. Among these eligible cases, 37 men (92.5%) agreed to participate after information was provided. Unilateral knee OA ($n = 21$) was more common than bilateral disease ($n = 16$). Among the 21 men with unilateral disease, OA tended to be right-sided ($n = 13$) more often

than left-sided (n = 8), but no significant difference was identified.

For controls, we approached age-, sex-, and residence-matched candidates for each case. To recruit the 37 matched controls, we approached 70 subjects (overall response rate 52.9%).

Table 1 shows background characteristics for the 37 case-control pairs in the present study. Mean body weight was significantly greater for cases than for controls ($P < 0.05$). Furthermore, body mass index was significantly higher for cases than for controls ($P < 0.05$). No differences in personal habits such as smoking or drinking were noted between cases and controls.

The association between knee OA and heaviest reported body weight was analyzed. Under univariate analysis, mean heaviest reported body weight for cases was 72.1 kg (standard deviation (SD) = 13.0 kg), significantly higher than that for controls ($P < 0.01$) in men. Odds ratios for heaviest reported body weight were 1.07 (95% CI 1.02–1.13), suggesting that a 1-kg increase in heaviest reported body weight raised the risk of knee OA by 7%.

To more clearly address the influence of heaviest reported weight on development of knee OA, cases were categorized into the following three groups according to the distribution of heaviest reported weight: high, ≥72.0 kg; middle, 61.0–72.0 kg; and low, <61.0 kg. These categories were defined by dividing total distributions into equal thirds. Cases in the high group displayed a >4-fold elevation in risk compared with cases in the low group (OR 4.22, 95% CI 1.13–15.8 for high vs low, $P < 0.05$; OR 1.60, 95% CI 0.50–5.08 for middle vs low, $P = 0.43$) (Fig. 1).

The association between knee OA and history of injury in other joints was calculated. Under univariate analysis, although ORs exceeded a 2-fold increase, no significant difference was observed between cases and controls (OR 2.50, 95% CI 0.78–7.97 for yes vs no, $P = 0.12$).

The association between knee OA and methods of transportation was examined by comparing the frequency of regular bicycle use between cases and controls. Under univariate analysis, while OR was higher for men (OR 2.67, 95% CI 0.71–10.05), no significant differences were noted between cases and controls.

Associations between knee OA and occupational history were analyzed. The most frequent areas of employment for all subjects were factory/construction, agriculture/fishery, clerical/technical, and shop assistant/manager (Table 2). Distributions of initial and principal occupations differed

Table 1. Anthropometric and background characteristics of cases and controls for knee OA in men

	Men	
	Cases	Controls
No. of participants	37	37
Age (years)	70.0 ± 6.6	70.1 ± 7.0
Weight (kg)	64.1 ± 10.7*	59.3 ± 8.7
Height (cm)	162.5 ± 6.9	163.0 ± 6.7
Body mass index (kg/m^2)	24.2 ± 3.4*	22.4 ± 3.8
Heaviest weight in the past (kg)	72.1 ± 13.0**	64.0 ± 9.2
Age at the heaviest weight (years)	57.4 ± 15.1*	51.7 ± 17.8
Current smoking (%)	16 (43.2)	15 (40.5)
Current drinking (≥5 times/week, %)	20 (54.1)	22 (59.5)

Mean ± SD; percentage in parentheses
* $P < 0.05$, ** $P < 0.01$ cases vs controls

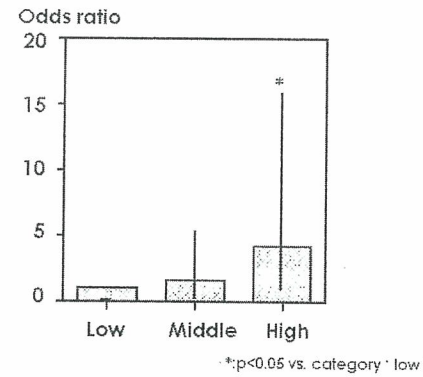

Fig. 1. Association of knee osteoarthritis with heaviest weight in the past. *Low*, lowest 3rd of the heaviest weight category, <61.0 kg; *Middle*, middle 3rd, ≥61.0 kg, <72.0 kg; *High*, highest 3rd, ≥72.0 kg. *Bar* represents 95% confidence interval

Table 2. Occupations reported as initial and principal jobs in men

	Initial occupation				Principal occupation			
	Cases	%	Controls	%	Cases	%	Controls	%
Total	37	100	37	100	37	100	37	100
Factory/construction workers	18	48.6	14	37.8	22	59.5	16	43.2
Agricultural/fishery workers	10	27.0	6	16.2	7	18.9	4	10.8
Clerical workers/technical experts	4	10.8	6	16.2	2	5.4	9	24.3
Shop assistants and managers	2	5.4	9	24.3	2	5.4	6	16.2
Clinical workers	2	5.4	0	0.0	1	2.7	0	0.0
Housekeepers	0	0.0	0	0.0	0	0.0	0	0.0
Hairdressers	0	0.0	0	0.0	0	0.0	0	0.0
Dressmakers	0	0.0	0	0.0	0	0.0	0	0.0
Teachers	0	0.0	0	0.0	2	5.4	0	0.0
Others (soldier, taxi driver, etc.)	1	2.7	2	5.4	1	2.7	2	5.4
No work, no answer	0	0.0	0	0.0	0	0.0	0	0.0

Table 3. Crude and adjusted odds ratios with risk factors for knee osteoarthritis in men

Men	Risk factors	Crude odds ratio (95% CI)	Adjusted odds ratio (95% CI)
Heaviest reported weight[a]	Middle vs Low	1.60 (0.50–5.08)	1.25 (0.29–5.35)
	High vs Low	4.22 (1.13–15.8)*	6.01 (1.18–30.5)*
Past injury of either knee	Yes vs No	2.50 (0.78–7.97)	6.25 (1.13–34.5)*
Occupational factors	Physical work[b] as principal occupation (vs Others)	2.80 (1.01–7.77)*	6.20 (1.40–27.5)*

Adjusted odds ratio refers to values after mutual adjustment for other potential risk estimates
95% CI, 95% confidence interval
[a] Lowest 3rd, <61.0 kg; middle 3rd, ≥61.0 kg, <72.0 kg; highest 3rd, ≥72.0 kg in men
[b] Physical work meaning factory, construction, agriculture or fishery work
* $P < 0.05$

Table 4. Crude and adjusted odds ratios with risk factors for knee osteoarthritis in women (cited from ref. 10)

Women	Risk factors	Crude odds ratio (95% CI)	Adjusted odds ratio (95% CI)
Heaviest reported weight[a]	Middle (vs Low)	1.68 (0.79–3.84)	3.33 (0.95–11.7)
	High (vs Low)	3.10 (1.26–7.98)*	3.92 (1.03–14.8)*
Past injury of either knee	Yes vs No	5.00 (2.44–10.2)*	7.51 (2.40–23.5)**
Transportation	Cycling almost every day for ≥12 months (vs Less)	1.88 (1.02–3.94)*	1.67 (0.61–4.57)
Occupational factors	Physical work[b] as initial occupation (vs Others)	2.54 (1.34–4.82)**	2.08 (0.88–5.61)
	Sitting ≥2 h/day at initial job (vs Less)	0.43 (0.23–0.78)**	0.44 (0.47–1.10)
	No. of jobs (1 job)	1.24 (1.02–1.50)*	0.91 (0.66–1.25)
	Total working period (1 year)	1.05 (1.03–1.07)***	1.05 (1.01–1.08)**

Adjusted odds ratio refers to values after mutual adjustment for other potential risk estimates
95% CI, 95% confidence interval
[a] Lowest 3rd, <55.0 kg; middle 3rd, ≥55.0 kg, <62.0 kg; highest 3rd, ≥62.0 kg in women
[b] Physical work meaning factory, construction, agriculture or fishery work
* $P < 0.05$; ** $P < 0.01$; *** $P < 0.001$

significantly between cases and controls. Physical work (factory/construction or agriculture/fishery) at the principal job was significantly more common among cases than controls (OR 2.80, 95% CI 1.01–7.77 for yes vs no). Mean age at commencement of the first job was 16.3 years (SD 3.8 years) compared to 16.6 years (SD 4.1 years) for controls, indicating no significant difference between cases and controls. Occupational activities including standing, climbing stairs, kneeling, squatting, driving, walking, sitting, and heavy lifting were not associated with increased risk of knee OA in men.

Table 3 shows ORs determined using conditional logistic regression analysis mutually adjusted for potential risk factors. Various risk factors were entered into the conditional logistic model, comprising: heaviest reported weight; previous knee injury; and physical work at the principal occupation in men. Heaviest reported weight in the past (OR 6.01, 95% CI 1.18–30.5, $P < 0.05$), past injury of the knee (OR 6.25, 95% CI 1.13–34.5, $P < 0.05$), and physical work at the principal occupation (OR 6.20, 95% CI 1.40–27.5, $P < 0.05$) represented independent factors associated with knee OA after controlling for other risk factors (Table 3).

Discussion

The results of the present case-control study indicate that heavy weight in the past and previous knee injury are associated with knee OA in men. Also in men, the proportion engaged in physical work (factory, construction, agriculture, or fishery work) was significantly higher among cases than controls. These risk factors for male knee OA are similar to those seen for female OA knees. Although we have already reported the results elsewhere,[10] we briefly compared results for men and women. Table 4 shows ORs in women determined using conditional logistic regression analysis mutually adjusted for potential risk factors. Various risk factors were entered into the conditional logistic model, comprising: heaviest reported weight in the past; previous knee injury; regular bicycle use; physical work in initial occupation; sedentary work in initial occupation; number of jobs; and total working period, summarizing all years of all jobs that subjects worked. Heaviest reported weight in the past, past injury of the knee, and total working period in women represented independent factors associated with knee OA after controlling for other risk factors. The results of the present case-control study indicate that heavy weight in the past and previous knee injury are associated with knee OA in both men and women.

Several limitations apply to the present study. Firstly, this investigation was based on a relatively small number of male cases and controls. Before the start of the research, we had calculated the sample size. We accumulated 155 pairs of cases and controls based on assumed values of a 0.05 level of significance, 80% statistical power, 2.0 risk ratio, and the 30% prevalence of cases. As a result, we succeeded in identifying 160 cases (40 men, 120 women) >45 years old

Table 5. Comparison of risk factors for hip and knee osteoarthritis (OA) in Britain and Japan (combined results for men and women)

	Risk factors	Britain	Japan
Hip OA	Obesity	Yes	No
	Past joint disturbance	Yes	No
	Occupational factors	Yes (lifting)	Yes (lifting)
Knee OA	Obesity	Yes	Yes
	Past joint disturbance	Yes	Yes
	Occupational factors	Yes (kneeling/squatting)	Yes (physical work, working period)

who fulfilled the entry criteria for the study. Of the eligible cases, 138 (86.3%; 37 men, 101 women) agreed to participate. However, the lack of gender balance for cases resulted in a small number of male subjects, which might reduce statistical power, and thus might not have detected other risk factors among lifestyle variables. This could be due to the use of identical case definitions for subject selection as the case-control hip OA and British studies. Cases were defined as those suffering knee pain and walking difficulties, who were first diagnosed by an orthopedic surgeon as displaying a tibiofemoral joint with a radiographic grade of ≥3 on the Kellgren and Lawrence scale. Our previous comparative study of OA in the lumbar spine indicated that OA in the general population tends to display lower prevalence and severity in Japan than in Britain.[14] In addition, the small number of male cases reflects gender differences in prevalence of knee OA in Japan. As a second limitation in the present study, the response rate for controls (52.8%) was lower than that for cases (92.0%). The present results may therefore be subject to some degree of overestimation.

Obesity has previously been shown to display strong associations with risk of knee OA,[2–8] and epidemiological studies performed in Japan have confirmed associations between obesity and knee OA.[15,16] In the present study, a history of heavy weight was shown to exert significant influences on risk of knee OA among men, resembling the results of women,[10] and consistent with previous studies. These findings indicate that the influence of heavy weight on knee OA is consistent across gender in both Japanese and Western populations.

The involvement of other joints is believed to play a role in increased risk of OA. In the British study paralleling the present study, presence of Heberden's node and previous knee injury were both strongly and independently associated with knee OA.[11,12] Although the present study did not seek information regarding the presence of Heberden's node, information was obtained about past history of the involvement of other joints and areas, as diagnosed by a medical doctor, indicating an independent association between previous knee injury and knee OA. In particular, site of knee OA was basically in accordance with the injured site among cases with previous knee injured (right side 91.7%, left side 100%). These findings were again consistent among men and women across Japanese and Western populations.

Mechanical stress represents another factor in the pathogenesis of OA at any joint site. In the present study, although occupational activities of standing, climbing stairs, kneeling, squatting, driving, walking, and heavy lifting were not associated with increased risk of knee OA in men, physical work at the principal occupation raised the risk of knee OA. Physical work represented by factory, construction, agricultural, or fishery work for long periods involved mechanical stress on the knee joints. The previous report utilized conditional logistic regression analysis without physical work, and identified sedentary work as a preventive factor in women.[10] These occupational activities influencing the risk of knee OA suggest that excess stress at the joint raises the risk, while reduced load on the joint decreases risk.

The present case-control study of knee OA paralleled our previous study of hip OA,[9] and was identical in format to some British studies.[17,18] Table 5 summarizes the results of studies using the same methods, indicating differences in risk factors between hip OA and knee OA, and between populations in Britain and Japan. Occupational factors clearly influence the development of both of hip and knee OA in Japan, as in Britain, although differences exist in specific activities exerting influence. Moreover, previous joint injury represented a risk factor for knee OA in Japan, as in the British studies. Conversely, obesity did not represent an independent risk factor for hip OA in Japan, but was a risk factor for both hip and knee OA in the British studies. This may be because local mechanical factors such as acetabular dysplasia might exert stronger influences on hip OA in Japan than other general mechanical factors such as adiposity. However, these results suggest that the pathogenesis of knee OA is similar in Japan and Western countries. Further studies of OA in other sites are required to characterize the risk profile in Japan.

Acknowledgments This research was supported by Grants-in-Aid for Scientific Research A11770200 from the Ministry of Education, Science, Sports and Culture in Japan, the Japan Society for the Promotion of Science, Research Society for Metabolic Bone Diseases, Japan, and the Arthritis Research Campaign, UK. We wish to acknowledge the generosity of surgeons and internists in Saiseikai Wakayama Hospital, Wakayama; Hori Hospital, Sennan; Nishioka Orthopaedic Hospital, Arita; Ryujin Clinic, Wakayama; Tamai Orthopaedic Hospital, Hannan; and Yamamoto Clinic, Shimotsu, Japan; and of Mrs. Sumiko Suzuri for help in locating participants for interviewing. The results of

this study were presented in 2001 at the British Society for Rheumatology XVIIIth Annual General Meeting.

References

1. Murray CJL, Lopez AD. The global burden of disease. Geneva: World Health Organization; 1997.
2. Anderson JJ, Felson DT. Factors associated with osteoarthritis of the knee and the first national health and nutrition examination survey (NHANES-I): evidence for an association with overweight, race and physical demands for work. Am J Epidemiol 1988;128: 179–89.
3. Felson DT. The epidemiology of knee osteoarthritis: results from the Framingham Osteoarthritis Study. Semin Arthritis Rheum 1990;20 Suppl 1:42–50.
4. Spector TD. The fat on the joint: osteoarthritis and obesity. J Rheumatol 1990;17:283–4.
5. Felson DT, Zhang Y, Anthony JM, Naimark A, Anderson JJ. Weight loss reduces the risk for symptomatic knee osteoarthritis in women. Ann Intern Med 1992;116:535–9.
6. Hochenburg MC, Lethbridge-Cejku M, Scott WW, Reichle R, Plato CC, Tobin JD. The association of body weight, body fatness and body fat distribution with osteoarthritis of the knee: data from the Baltimore longitudinal study of aging. J Rheumatol 1995;22: 488–93.
7. Hart DJ, Doyle DV, Spector TD. Incidence and risk factors for radiographic knee osteoarthritis in middle-aged women: the Chingford Study. Arthritis Rheum 1999;42:17–24.
8. Cooper C, Snow S, McAlindon RW, Kellingray S, Stuart B, Coggon D, et al. Risk factors for the incidence and progression of radiographic knee osteoarthritis. Arthritis Rheum 2000;43:995–1000.
9. Yoshimura N, Sasaki S, Iwasaki K, Danjoh S, Kinoshita H, Yasuda T, et al. Occupational lifting is associated with hip osteoarthritis: a Japanese case-control study. J Rheumatol 2000;27: 434–40.
10. Yoshimura N, Nishioka S, Kinoshita H, Hori N, Nishioka T, Ryujin M, et al. Risk factors for knee osteoarthritis in Japanese women: heavy weight, past joint injuries and occupational activities. J Rheumatol 2004;31:157–62.
11. Cooper C, McAlindon T, Coggon D, Egger P, Dieppe P. Occupational activity and osteoarthritis of the knee. Ann Rheum Dis 1994;53:90–3.
12. Coggon D, Croft P, Kellingray S, Barrett D, McLaren M, Cooper C. Occupational physical activities and osteoarthritis of the knee. Arthritis Rheum 2000;43:1443–9.
13. Kellgren JH, Lawrence JS. Radiological assessment of osteoarthritis. Ann Rheum Dis 1957;16:494–502.
14. Yoshimura N, Dennison E, Wilman C, Hashimoto T, Cooper C. Epidemiology of chronic disc degeneration and osteoarthritis of the lumbar spine in Britain and Japan: a comparative study. J Rheumatol 2000;27:429–33.
15. Tamaki M, Koga Y. Osteoarthritis of the knee joint: a field study (in Japanese). Nippon Seikeigeka Gakkai Zasshi (J Jpn Orthop Assoc) 1994;68:737–50.
16. Suematsu N, Onozawa T, Suzuki S, Takemitsu Y, Niinuma R. Epidemiologic study of osteoarthritis of the knee in agricultural and forestry workers (in Japanese). Seikei Saigai Geka (Orthop Surg Traumatol) 1986;29:343–6.
17. Cooper C, Inskip H, Croft P, Campbell L, Smith G, McLaren M, et al. Individual risk factors for hip osteoarthritis; obesity, hip injury, and physical activity. Am J Epidemiol 1998;147:516–22.
18. Coggon D, Kellingray S, Inskip H, Croft P, Campbell L, Cooper C. Osteoarthritis of the hip and occupational lifting. Am J Epidemiol 1998;147:523–8.

nature medicine

LETTERS

Carminerin contributes to chondrocyte calcification during endochondral ossification

Takashi Yamada[1], Hirotaka Kawano[1], Yu Koshizuka[1], Toru Fukuda[2], Kimihiro Yoshimura[2], Satoru Kamekura[1], Taku Saito[1], Toshiyuki Ikeda[1], Yosuke Kawasaki[1], Yoshiaki Azuma[3], Shiro Ikegawa[4], Kazuto Hoshi[1], Ung-il Chung[1], Kozo Nakamura[1], Shigeaki Kato[2] & Hiroshi Kawaguchi[1]

Endochondral ossification is an essential process not only for physiological skeletal development and growth, but also for pathological disorders. We recently identified a novel cartilage-specific molecule, carminerin (also known as cystatin 10 and encoded by *Cst10*), which is upregulated in synchrony with cartilage maturation and stimulates the later differentiation of cultured chondrocytes[1]. Although carminerin-deficient (*Cst10*$^{-/-}$) mice developed and grew normally, they had a microscopic decrease in the calcification of hypertrophic chondrocytes at the growth plate. When we created experimental models of pathological endochondral ossification, we observed suppression of chondrocyte calcification during formation of osteoarthritic osteophytes, age-related ectopic ossification and healing of bone fractures in *Cst10*$^{-/-}$ mice. Cultured *Cst10*$^{-/-}$ chondrocytes showed a reduction in calcification with activation of an SRY site in the promoter of the gene encoding nucleotide pyrophosphatase phosphodiesterase 1 (NPP1, encoded by *Enpp1*). Functional NPP1 is required for carminerin deficiency to suppress the pathological endochondral ossifications listed above. Carminerin is the first cartilage-specific protein that contributes to chondrocyte calcification during endochondral ossification under physiological and pathological conditions through the transcriptional inhibition of NPP1.

We generated *Cst10*$^{-/-}$ mice by homologous recombination in mouse embryonic stem cells using a targeting vector to replace exon 1 with the phosphoglycerate kinase-neomycin (PGKneo) cassette (**Fig. 1a**). Inbreeding of heterozygous *Cst10*$^{+/-}$ mice yielded *Cst10*$^{-/-}$ mice, as determined by Southern blot analysis, at the expected mendelian ratio (**Fig. 1b**). Neither *Cst10* transcripts nor carminerin protein was detected in the rib cartilage of *Cst10*$^{-/-}$ mice, confirming disruption of the *Cst10* gene (**Fig. 1c,d**). *Cst10*$^{-/-}$ mice developed and grew similarly to wild-type (*Cst10*$^{+/+}$) and *Cst10*$^{+/-}$ littermates without abnormalities of major organs (**Fig. 1e,f**).

Radiological analyses of femurs and tibiae in 8-week-old mice showed that *Cst10*$^{-/-}$ mice experienced decreases in trabecular bone volume mainly at the metaphysis, but not in cortical bone at the diaphysis, as compared to the wild-type littermates (**Fig. 2a,b** and **Supplementary Fig. 1** online). Histological examination of the proximal tibias indicated a decrease in trabecular bone volume beneath the growth plate of *Cst10*$^{-/-}$ mice (**Fig. 2c**). Although expression of carminerin was localized mainly in the wild-type hypertrophic chondrocytes, the columnar architecture, expression of type X collagen (Col X) and the entire width of the growth plate were comparable between wild-type and *Cst10*$^{-/-}$ mice, indicating that hypertrophic differentiation of chondrocytes was not affected by the carminerin deficiency (**Fig. 2c,d**). The width of the calcified layer and the number of calcified chondrocytes, as determined by von Kossa staining, however, were reduced (**Fig. 2c,d**). Bone volume in the *Cst10*$^{-/-}$ primary spongiosa just beneath the growth plate was significantly reduced ($P < 0.01$), with normal numbers of tartrate-resistant acid phosphatase (TRAP)-positive chondroclasts or osteoclasts, whereas the secondary spongiosa was not affected (**Fig. 2c,d** and **Supplementary Fig. 1**). In vertebral bodies that undergo less longitudinal growth by the thinner growth plate than femurs and tibiae, the histomorphometric parameters were comparable between the two genotypes in the growth plate and the primary and secondary spongiosa (**Supplementary Fig. 1**). These findings indicate that the decrease in trabecular bone adjacent to the growth plate of *Cst10*$^{-/-}$ long bones under physiological conditions resulted primarily from impairment of the calcification of hypertrophic chondrocytes, but not from the abnormality of cartilage resorption by chondroclasts or bone formation by osteoblasts.

We then examined the involvement of carminerin in pathological endochondral ossification by using experimental models involving wild-type and *Cst10*$^{-/-}$ littermates. First, we investigated the role of carminerin in the pathogenesis of osteoarthritis by inducing instability in the mouse knee joint[2]. The joint cartilage destruction was similarly visible at the posterior of the tibias (**Fig. 3a**) in both genotypes. The

[1]Department of Sensory & Motor System Medicine, Faculty of Medicine, University of Tokyo, Hongo 7-3-1, Bunkyo, Tokyo 113-8655, Japan. [2]Institute of Molecular and Cellular Biosciences, University of Tokyo, Yayoi 1-1-1, Bunkyo, Tokyo 113-0032, Japan. [3]Teijin Institute for Biomedical Research, Asahigaoka 4-3-2, Hino, Tokyo 191-8512, Japan. [4]Institute of Physical and Chemical Research (RIKEN), Shirokanedai, Minato, Tokyo 106-8639, Japan. Correspondence should be addressed to H.K. (kawaguchi-ort@h.u-tokyo.ac.jp).

Received 1 January; accepted 7 April; published online 7 May 2006; doi:10.1038/nm1409

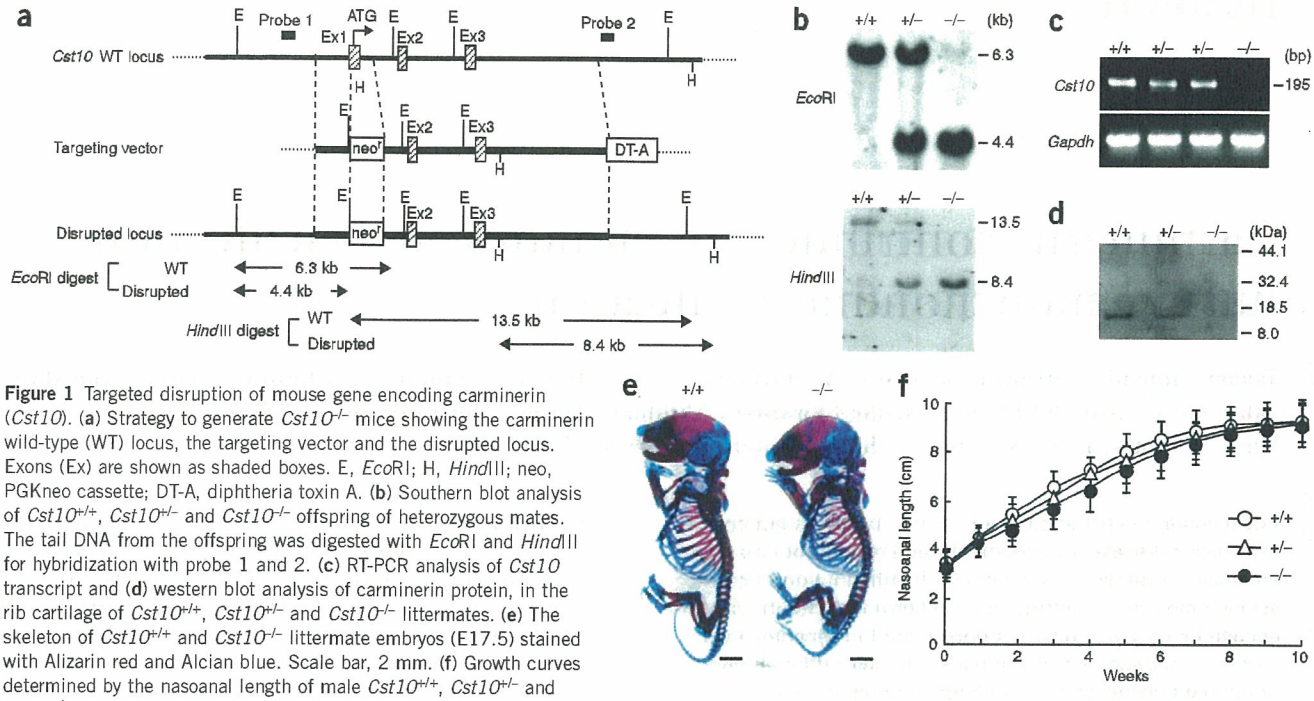

Figure 1 Targeted disruption of mouse gene encoding carminerin (*Cst10*). (**a**) Strategy to generate *Cst10*$^{-/-}$ mice showing the carminerin wild-type (WT) locus, the targeting vector and the disrupted locus. Exons (Ex) are shown as shaded boxes. E, *Eco*RI; H, *Hind*III; neo, PGKneo cassette; DT-A, diphtheria toxin A. (**b**) Southern blot analysis of *Cst10*$^{+/+}$, *Cst10*$^{+/-}$ and *Cst10*$^{-/-}$ offspring of heterozygous mates. The tail DNA from the offspring was digested with *Eco*RI and *Hind*III for hybridization with probe 1 and 2. (**c**) RT-PCR analysis of *Cst10* transcript and (**d**) western blot analysis of carminerin protein, in the rib cartilage of *Cst10*$^{+/+}$, *Cst10*$^{+/-}$ and *Cst10*$^{-/-}$ littermates. (**e**) The skeleton of *Cst10*$^{+/+}$ and *Cst10*$^{-/-}$ littermate embryos (E17.5) stained with Alizarin red and Alcian blue. Scale bar, 2 mm. (**f**) Growth curves determined by the nasoanal length of male *Cst10*$^{+/+}$, *Cst10*$^{+/-}$ and *Cst10*$^{-/-}$ mice. Data are expressed as mean ± s.e.m. for 15 mice per group. Females also showed similar skeletal development and growth in all genotypes.

carminerin expression was colocalized with Col X in the wild-type hypertrophic chondrocytes adjacent to the osteophyte (**Fig. 3b**). Although the hypertrophic differentiation of chondrocytes was not affected by the carminerin deficiency (**Fig. 3a**), osteophyte formation at the posterior of the tibias was significantly decreased (**Fig. 3a,c**). These findings confirmed by quantification by the Mankin grading score[3] and the osteophyte volume (**Fig. 3d**) indicate that carminerin produced in hypertrophic chondrocytes as a result of mechanical stress contributes to osteophyte formation through chondrocyte calcification, without affecting cartilage destruction or chondrocyte hypertrophy.

Similar findings were observed in ectopic ossification of the patellar ligament and the Achilles tendon with aging (**Supplementary Methods** online), which was significantly decreased by the carminerin deficiency ($P < 0.05$; **Supplementary Fig. 2** online). The colocalization of Col X and carminerin adjacent to the ectopic ossification indicates the involvement of carminerin-expressing hypertrophic chondrocytes in this disorder as well (**Supplementary Fig. 2**).

We further examined the involvement of carminerin in bone fracture healing at the midshaft of tibias[4,5]. *Cst10*$^{-/-}$ mice showed a bone gap upon X-ray 3 weeks after the fracture, with substantial formation of cartilaginous callus but impaired calcification, especially at the central area (**Fig. 4a**). Again, carminerin was expressed in the wild-type chondrocytes adjacent to the calcified callus. The time course of bone mineral content (BMC) showed that calcification in the central one-third portion, but not in the peripheral two-thirds portion, was significantly reduced during the endochondral ossification period (2–7 weeks after fracture) in the *Cst10*$^{-/-}$ callus, although bone union was eventually achieved from the *Cst10*$^{-/-}$ small callus through unaffected bone formation and remodeling thereafter (**Fig. 4b**). This model also indicates that the carminerin deficiency impaired endochondral ossification, but not intramembranous ossification or osteoblastic bone formation.

The effects of carminerin deficiency on endochondral ossification under the pathological conditions above were more obvious than those under physiological conditions, which showed only a microscopic change. The phenotype of the physiological *Cst10*$^{-/-}$ growth plate was milder than that seen in other disorders such as vitamin A deficiency, which causes not only impaired chondrocyte calcification but also insufficient resorption of unmineralized cartilage by chondroclasts, leading to a suppressed skeletal growth[6]. The difference may be caused by operation of compensatory mechanisms for endochondral ossification, including osteoblastic bone formation and remodeling unaffected by the carminerin deficiency, which are sufficient to compensate for the deficiency under physiological conditions, but not so under pathological conditions.

Carminerin was originally called cystatin 10 because its amino acid sequence contained similarity to the cystatin protein family; however, our examination has not detected legitimate cystatin activity, which inhibits cysteine proteinases (**Supplementary Table 1** and **Supplementary Methods** online). We therefore renamed this protein carminerin after 'cartilage mineralization'. To elucidate the actual mechanism of carminerin action on endochondral ossification, we compared *ex vivo* cultures of chondrocytes isolated from the growth plates of the wild-type and *Cst10*$^{-/-}$ tibias (**Supplementary Methods**). Although chondrocyte proliferation and differentiation were similar between the two genotypes, chondrocyte calcification was suppressed in the *Cst10*$^{-/-}$ culture (**Supplementary Fig. 3** online), indicating a cell-autonomous effect. In contrast, *ex vivo* cultures of primary osteoblasts obtained from wild-type and *Cst10*$^{-/-}$ calvariae confirmed that these cells do not express carminerin, so that there was no difference of bone formation by osteoblasts in this bone type (**Supplementary Fig. 3**).

As inorganic pyrophosphate (PPi) is known to be a crucial inhibitor of calcification[7], we compared the expression of a few molecules that

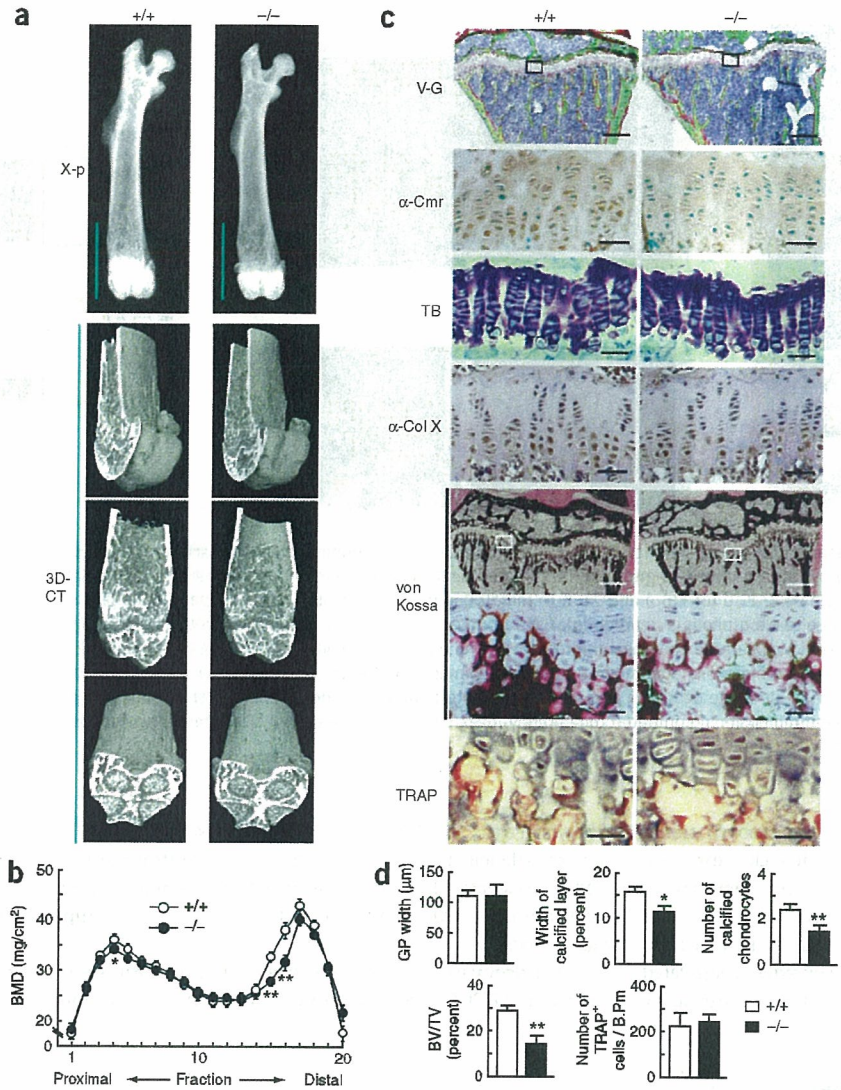

Figure 2 Radiological and histological findings of the long bones in wild-type (*Cst10*$^{+/+}$) and *Cst10*$^{-/-}$ littermates at 8 weeks of age under physiological conditions. (**a**) Plain X-ray of whole femurs, and three-dimensional computed tomography images of the distal part shown as green lines on the plain X-ray. (**b**) Bone mineral density (BMD) of the 20 equally divided fractions of femurs. (**c**) Histological findings of the proximal tibias. Villanueva-Goldner staining (V-G; scale bar, 200 μm). Inset boxes indicate the regions of the following three rows: immunostaining with an antibody to carminerin (α-Cmr; scale bar, 20 μm), toluidine blue staining (TB; scale bar, 20 μm), immunostaining with an antibody to Col X (α-Col X; scale bar, 20 μm). von Kossa staining (scale bars, 200 μm (top) and 20 μm (bottom)). Inset boxes indicate the regions of the bottom two rows: von Kossa staining and TRAP staining (scale bar, 20 μm). (**d**) Histomorphometric analyses of the growth plate and primary spongiosa just beneath it. The entire growth plate width (GP width) was measured on the TB sections, and the percent width of calcified layer to the entire growth plate and the number of calcified chondrocytes per column were measured on the von Kossa sections. Bone volume/tissue volume (BV/TV) and the number of TRAP^{+} cells in 100 mm of bone perimeter were measured in the primary spongiosa. Data are expressed as mean ± s.e.m. for 15 mice per group. $^{*}P < 0.05$, $^{**}P < 0.01$ compared to wild-type mice.

control the level of PPi in the cultured growth-plate chondrocytes, including: NPP1, which generates PPi from nucleoside triphosphates using nucleoside triphosphate pyrophosphohydrolase (NTPPPH) activity[8], tissue-nonspecific alkaline phosphatase (TNAP) which hydrolyzes PPi[9], and the multiple-pass transmembrane protein ANK, which mediates intracellular-to-extracellular channeling of PPi[10]. Among these proteins, the carminerin deficiency upregulated expression of only NPP1, and accordingly, increased NTPPPH activity (**Supplementary Fig. 3**). The reintroduction of carminerin into *Cst10*$^{-/-}$ chondrocytes (Ax-*Cmr*) restored the abnormalities in calcification, expression of NPP1 and NTPPPH activity to those similar to the wild-type culture (**Supplementary Fig. 3**). The promoter activity of an *Enpp1* promoter-luciferase construct (–964 *Enpp1* promoter-Luc) transfected into ATDC5 cells overexpressing carminerin (pCMV-*Cmr*/ATDC5) was lower than cells transfected with mock vector (pCMV/ATDC5; **Supplementary Fig. 3**). Deletion analysis of the *Enpp1* promoter region identified the core responsive element between the –360 and –324 regions, within which an SRY (sex-determining region Y) consensus sequence was predicted. Site-directed mutagenesis to eliminate the SRY site canceled the inhibition of *Enpp1* transcription by carminerin. Electrophoretic mobility shift assay confirmed specific binding of the SRY region by an oligonucleotide probe with nuclear extracts prepared from pCMV/ATDC5 and pCMV-*Cmr*/ATDC5 cells. Binding by the probe was weaker with the pCMV-*Cmr*/ATDC5 extracts than with the pCMV/ATDC5 extracts (**Supplementary Fig. 3**). As the binding was not detected using the synthetic carminerin protein instead of the nuclear extracts, carminerin itself was shown not to be the direct transcription factor for the SRY region. In contrast, nuclear extracts from the primary *Cst10*$^{-/-}$ growth plate chondrocytes showed stronger binding with the SRY site than those from the wild-type chondrocytes (**Supplementary Fig. 3**). Hence, the transcriptional inhibition of NPP1 expression by carminerin may result, at least partly, from the impaired binding of a transcription factor to the SRY site of the *Enpp1* promoter. Although Sox9, a potent regulator of chondrocyte differentiation[11,12], is the most probable transcription factor for this site, we did not observe a supershift of the DNA-protein complex when we added Sox9-specific antibody in the electrophoretic mobility shift assay (data not shown), indicating the involvement of other transcription factors in the regulation of the SRY site. In addition, in our efforts to identify the upstream regulator of NPP1, we did not find substantial regulation of expression or transcription of NPP1 by carminerin through the cytokines interleukin-1β (IL-1β), fibroblast growth factor-2 (FGF-2) or transforming growth factor-β (TGF-β), which previously have been reported to regulate NPP1 expression[13–15] (**Supplementary Fig. 4** online). Thus, further studies to elucidate a more detailed mechanism through which carminerin inhibits transcription of NPP1 will be necessary.

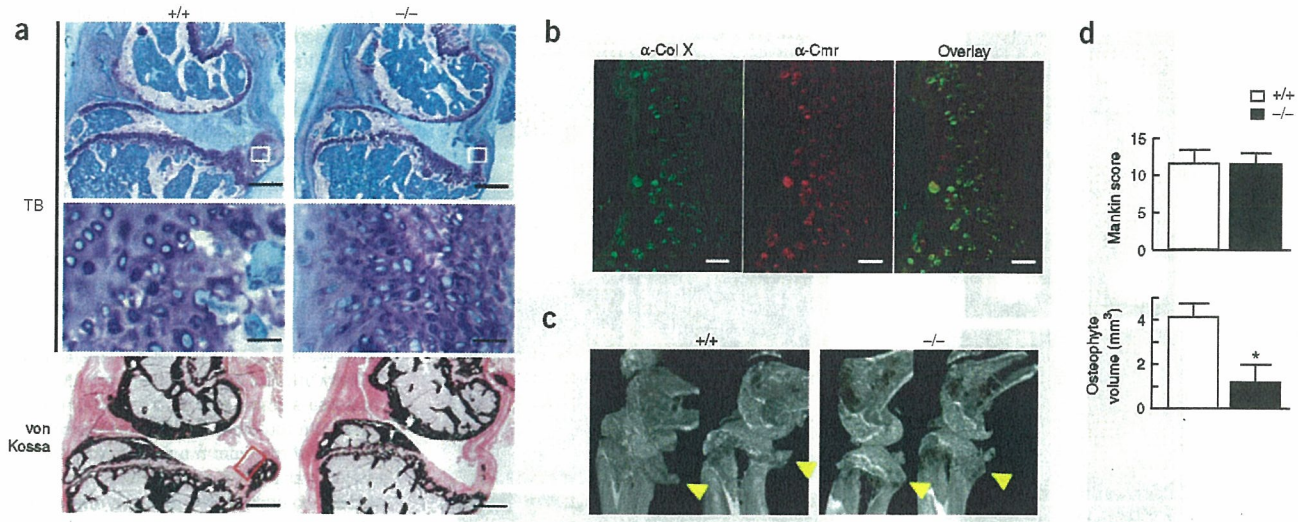

Figure 3 Histological and radiological findings of osteoarthritic joints in wild-type (*Cst10*$^{+/+}$) and *Cst10*$^{-/-}$ littermates. (**a**) Osteoarthritis was induced at the posterior tibias of the knee joint of 8-week-old mice by surgically imposing instability to the joint. Histological features; toluidine blue (TB; inset boxes in the top figures indicate regions shown in middle row; scale bars, 200 μm (top) and 20 μm (middle)) and von Kossa stainings (scale bar, 200 μm) of the sagittal sections of knee joints 10 weeks after surgery (left side of each photo is anterior side). (**b**) Immunostainings with an antibody to Col X (α-Col X, green), an antibody to carminerin (α-Cmr, red) and the overlay (yellow) analyzed by confocal microscopy in the region indicated in the inset of the image of von Kossa staining of wild-type knee in **a**. Scale bar, 20 μm. (**c**) Three-dimensional computed tomography images of the knee joints from the posterolateral projection. Arrowheads indicate osteophytes. (**d**) Quantification of the cartilage destruction and the osteophyte formation as determined by the Mankin grading score (top) and the osteophyte volume measured on the three-dimensional computed tomography images (bottom), respectively. Data are expressed as mean ± s.e.m. for ten mice per group. $^{*}P < 0.01$ compared to wild-type mice.

Finally, we carried out *in vitro* fertilization and embryo transfer from *Cst10*$^{-/-}$ mice and the *Enpp1*$^{-/-}$ mice, which lack expression of functional NPP1 (ref. 16), and generated four genotypes of mice: *Cst10*$^{+/+}$*Enpp1*$^{+/+}$, *Cst10*$^{-/-}$*Enpp1*$^{+/+}$, *Cst10*$^{+/+}$*Enpp1*$^{-/-}$ and *Cst10*$^{-/-}$*Enpp1*$^{-/-}$. When we used the experimental models, there was no difference in formation of osteoarthritic osteophytes, age-related ectopic ossification or high phosphate–induced auricular ossification between the NPP1-deficient mice (*Cst10*$^{+/+}$*Enpp1*$^{-/-}$) and the double-deficient mice (*Cst10*$^{-/-}$*Enpp1*$^{-/-}$), confirming that functional NPP1 is essential for suppression of the pathological endochondral ossification by the carminerin deficiency *in vivo* (**Supplementary Fig. 5** online).

Our previous *in vitro* study showed that overexpression of carminerin in ATDC5 cells accelerated not only calcification but also

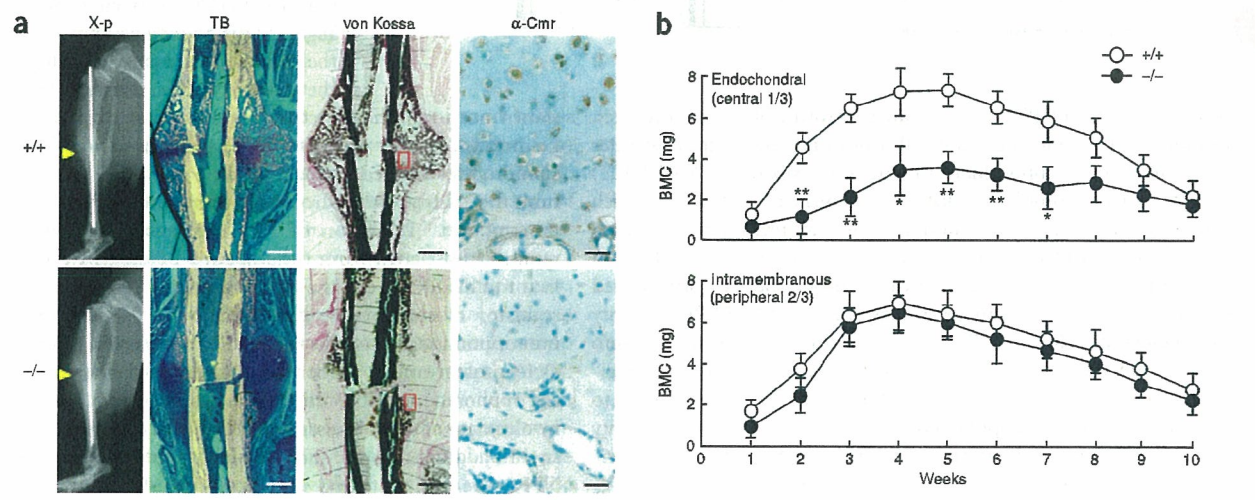

Figure 4 Radiological and histological findings of bone fracture healing in wild-type (*Cst10*$^{+/+}$) and *Cst10*$^{-/-}$ littermates. Fracture was produced by a transverse osteotomy that was stabilized with an intramedullary nail at the midshaft of tibias in 8-week-old mice. (**a**) Plain X-ray, toluidine blue (TB), von Kossa and a carminerin-specific antibody (α-Cmr) immunostainings 3 weeks after fracture. Insets in the image of von Kossa staining indicate regions of immunostaining. Scale bar, 20 μm for immunostaining, and 200 μm for the others. (**b**) Time course of bone mineral content (BMC) at the fracture callus for 10 weeks after fracture. BMC of the central one-third portion was measured as the endochondral ossification, and BMC of the peripheral two-thirds as the intramembranous ossification. Data are expressed as mean ± s.e.m. for six mice per time per group. $^{*}P < 0.05$, $^{**}P < 0.01$ compared to wild-type mice.

hypertrophic differentiation[1]. In contrast, the present *in vivo* and *in vitro* studies on deficiency of carminerin showed no abnormality in hypertrophic differentiation of chondrocytes. This discrepancy might owe to the involvement of insulin signaling by way of NPP1 regulation because in addition to the enzymatic function of synthesizing PPi, NPP1 is known to suppress the tyrosine kinase activity of the insulin receptor[17]. Considering that our previous ADTC5 cell culture was carried out in the presence of insulin (10 μg/ml), which was essential to induce hypertrophic differentiation[18], overexpression of carminerin might cause suppression of NPP1, which in turn increases sensitivity to insulin and enhances hypertrophic differentiation. The fact that the serum insulin levels in wild-type and *Cst10*$^{-/-}$ mice were similar (0.32 ± 0.08 and 0.35 ± 0.06 ng/ml, respectively; mean ± s.e.m. of five mice per genotype) and were much lower than the *in vitro* concentration, indicates that the regulation of chondrocyte calcification by endogenous carminerin *in vivo* was not mediated by insulin signaling.

Pi has been suggested to be rate limiting for calcification, which may explain why clinical disorders in homeostasis of Pi lead to, for example, rickets, osteomalacia[19] and ectopic calcification[20]. Considering that carminerin was isolated as a protein that was upregulated by a high-phosphate diet in association with calcification of mouse auricular cartilage, carminerin might partly mediate Pi-induced cartilage calcification. In fact, carminerin deficiency decreased calcification of auricular cartilage in wild-type mice on a high-phosphate diet (**Supplementary Fig. 5**). Carminerin may therefore be the first cartilage-specific protein that induces chondrocyte calcification during endochondral ossification under physiological and pathological conditions.

METHODS

Generation of *Cst10*$^{-/-}$ mice. We obtained a *Cst10* genomic clone by screening a bacterial artificial chromosome (BAC) library using a BAC PCR screening system (Genome Systems). We used a 120-kb fragment of a BAC clone containing all exons (1–3) of *Cst10* to construct the targeting vector. We constructed the targeting vector to replace exon 1, including the transcription initiation site, by the neomycin-resistance gene. We introduced the linearized targeting vector by electroporation into embryonic stem (ES) cells as previously described[21], and identified two independent targeted ES cell clones by Southern blot analysis, using 5′ (probe 1) and 3′ (probe 2) external probes. We generated chimeric males and crossed them with C57BL/6 females, and verified germline transmission by Southern blot analysis. All *Cst10*$^{-/-}$ mice used in this study had been backcrossed for ten generations into the C57BL/6 background. We used RT-PCR to determine the presence of the *Cst10* transcripts. We determined presence of carminerin protein by western blot analysis, as previously described, using a polyclonal antibody to the full-length carminerin protein, which was raised in rabbits using a synthetic peptide of carminerin[1].

Mice conditions. We fed mice a standard rodent diet (CE-2; CLEA Japan) or a high-phosphate diet containing 1.86% phosphorus. In each experiment, we compared littermate wild-type and *Cst10*$^{-/-}$ mice generated from the intercross between heterozygous mice. All experiments were performed on male mice, according to the protocol approved by the Animal Care and Use Committee of the University of Tokyo.

Skeletal preparations. We fixed whole skeletons of wild-type and *Cst10*$^{-/-}$ littermate embryos (E17.5) in 99.5% ethanol, transferred them into acetone and stained them as previously described[21]. We kept specimens in 20% glycerol-1% KOH until skeletons became clearly visible.

Radiological analyses. We took plain radiographs using a soft X-ray apparatus. We measured the bone mineral density (BMD) of the 20 equally divided fractions of the entire femur and bone mineral content (BMC) of the fracture callus with dual energy X-ray absorptiometry using a bone mineral analyzer. We carried out micro–computed tomography scanning using a composite X-ray analyzer, and reconstructed cross-sectional tomograms of 10 μm thickness at 12 × 12 pixels into a three-dimensional feature by the volume-rending method; we then measured the ossification volume using a computer. We performed peripheral quantitative computed tomography scans at the metaphysis of 0.2 mm below the proximal growth plate and at the midshaft of tibias.

Histological analyses. For Villanueva-Goldner, toluidine blue and von Kossa stainings, we fixed samples with 70% ethanol, embedded them in glycol methacrylate without decalcification and sectioned them into 3-μm slices. We carried out histomorphometric analyses in the growth plate, primary spongiosa just beneath it (0.3 mm in length) and secondary spongiosa (1.0 mm in length from 0.3 mm below the growth plate) of the proximal tibias and the fifth vertebra using an image analyzer. For double labeling to analyze the dynamic bone remodeling, we subcutaneously injected mice with 8 mg/kg body weight of calcein at 10 d and 3 d before killing. We stained TRAP^{+} cells at pH 5.0 in the presence of L(+)-tartaric acid using naphthol AS-MX phosphate in *N,N*-dimethyl formamide as the substrate. We performed histomorphometric measurements in eight optical fields, according to the American Society for Bone and Mineral Research nomenclature report[22], and calculated the averages per mouse. For H&E staining, we perfused mice with 4% buffered paraformaldehyde, decalcified bones with 4.13% EDTA, embedded them in paraffin, and cut them into 6 μm–thick sections. For immunohistochemical analyses, we treated sections as previously described[4], using polyclonal rabbit antibody to carminerin or Col X (Santa Cruz Biotechnology). For double staining, we treated sections with 1% BSA, incubated them with a mixture of carminerin-specific antibody and mouse monoclonal Col X–specific antibody and with Texas red-conjugated goat antibody to rabbit IgG. They were then reacted with biotin-conjugated antibodies to mouse IgG+IgA+IgM and FITC-streptoavidin. The localizations were observed by confocal laser scanning microscopy.

Osteoarthritis model. Eight-week-old mice underwent a microsurgery to produce instability in the knee joints as we reported previously[2]. Mice were killed 10 weeks after surgery, and cartilage destruction was quantified as the Mankin grading score[3] of the most severe change among multiple serial toluidine blue sections in each mouse. We measured osteophyte volume with three-dimensional computed tomography as described above.

Fracture model. We produced fracture at the midshaft of tibias of 8-week-old mice as we reported previously[4,5]. Several mice were killed each week for 10 weeks after the surgery. After the entire callus was longitudinally divided into three equal portions on a bone mineral analyzer image, we measured BMC at the central one-third portion as the endochondral ossification and that at the peripheral two-thirds as the intramembranous ossification. We performed histological analyses 3 weeks after fracture.

Statistical analysis. All data are expressed as mean ± s.e.m. Means of groups were compared by ANOVA and significance of differences was determined by *post hoc* testing using the Bonferroni method.

Note: Supplementary information is available on the Nature Medicine website.

ACKNOWLEDGMENTS

This study was supported by a Grant-in-aid for Scientific Research from the Japanese Ministry of Education, Culture, Sports, Science, and Technology (#14370454), and by the Investigation Committee on the Ossification of Spinal Ligaments, Japanese Ministry of Public Health and Welfare.

COMPETING INTERESTS STATEMENT

The authors declare that they have no competing financial interests.

Published online at http://www.nature.com/naturemedicine/
Reprints and permissions information is available online at http://npg.nature.com/reprintsandpermissions/

1. Koshizuka, Y. *et al.* Cystatin 10, a novel chondrocyte-specific protein, may promote the last steps of the chondrocyte differentiation pathway. *J. Biol. Chem.* **278**, 48259–48266 (2003).
2. Kamekura, S. *et al.* Osteoarthritis development in novel experimental mouse models induced by knee joint instability. *Osteoarthritis Cartilage* **13**, 632–641 (2005).

3. Mankin, H.J., Johnson, M.E. & Lippiello, L. Biochemical and metabolic abnormalities in articular cartilage from osteoarthritic human hips. III. Distribution and metabolism of amino sugar-containing macromolecules. *J. Bone Joint Surg. Am.* **63**, 131–139 (1981).
4. Shimoaka, T. *et al.* Impairment of bone healing by insulin receptor substrate-1 deficiency. *J. Biol. Chem.* **279**, 15314–15322 (2004).
5. Chikuda, H. *et al.* Cyclic GMP-dependent protein kinase II is a molecular switch from proliferation to hypertrophic differentiation of chondrocytes. *Genes Dev.* **18**, 2418–2429 (2004).
6. Wolbach, S.B. Vitamin-A deficiency and excess in relation to skeletal growth. *J. Bone Joint Surg.* **29**, 171–192 (1947).
7. Terkeltaub, R.A. Inorganic pyrophosphate generation and disposition in pathophysiology. *Am. J. Physiol. Cell Physiol.* **281**, C1–C11 (2001).
8. Bollen, M., Gijsbers, R., Ceulemans, H., Stalmans, W. & Stefan, C. Nucleotide pyrophosphatases/phosphodiesterases on the move. *Crit. Rev. Biochem. Mol. Biol.* **35**, 393–432 (2000).
9. Balcerzak, M. *et al.* The roles of annexins and alkaline phosphatase in mineralization process. *Acta Biochim. Pol.* **50**, 1019–1038 (2003).
10. Ryan, L.M. The ank gene story. *Arthritis Res.* **3**, 77–79 (2001).
11. de Crombrugghe, B., Lefebvre, V. & Nakashima, K. Regulatory mechanisms in the pathways of cartilage and bone formation. *Curr. Opin. Cell Biol.* **13**, 721–727 (2001).
12. Akiyama, H., Chaboissier, M.C., Martin, J.F., Schedl, A. & de Crombrugghe, B. The transcription factor Sox9 has essential roles in successive steps of the chondrocyte differentiation pathway and is required for expression of Sox5 and Sox6. *Genes Dev.* **16**, 2813–2828 (2002).
13. Lotz, M. *et al.* Interleukin 1 beta suppresses transforming growth factor-induced inorganic pyrophosphate (PPi) production and expression of the PPi-generating enzyme PC-1 in human chondrocytes. *Proc. Natl. Acad. Sci. USA* **92**, 10364–10368 (1995).
14. Solan, J.L., Deftos, L.J., Goding, J.W. & Terkeltaub, R.A. Expression of the nucleoside triphosphate pyrophosphohydrolase PC-1 is induced by basic fibroblast growth factor (bFGF) and modulated by activation of the protein kinase A and C pathways in osteoblast-like osteosarcoma cells. *J. Bone Miner. Res.* **11**, 183–192 (1996).
15. Oyajobi, B.O., Caswell, A.M. & Russell, R.G. Transforming growth factor beta increases ecto-nucleoside triphosphate pyrophosphatase activity of human bone-derived cells. *J. Bone Miner. Res.* **9**, 99–109 (1994).
16. Okawa, A. *et al.* Mutation in Npps in a mouse model of ossification of the posterior longitudinal ligament of the spine. *Nat. Genet.* **19**, 271–273 (1998).
17. Goldfine, I.D., Maddux, B.A., Youngren, J.F., Trischitta, V. & Frittitta, L. Role of PC-1 in the etiology of insulin resistance. *Ann. NY Acad. Sci.* **892**, 204–222 (1999).
18. Shukunami, C. *et al.* Chondrogenic differentiation of clonal mouse embryonic cell line ATDC5 *in vitro*: differentiation-dependent gene expression of parathyroid hormone (PTH)/PTH-related peptide receptor. *J. Cell Biol.* **133**, 457–468 (1996).
19. Laroche, M. Phosphate, the renal tubule, and the musculoskeletal system. *Joint Bone Spine* **68**, 211–215 (2001).
20. Jono, S. *et al.* Phosphate regulation of vascular smooth muscle cell calcification. *Circ. Res.* **87**, E10–E17 (2000).
21. Nakamichi, Y. *et al.* Chondromodulin I is a bone remodeling factor. *Mol. Cell. Biol.* **23**, 636–644 (2003).
22. Parfitt, A.M. *et al.* Bone histomorphometry: standardization of nomenclature, symbols, and units. Report of the ASBMR Histomorphometry Nomenclature Committee. *J. Bone Miner. Res.* **2**, 595–610 (1987).

Magnetic targeting of bone marrow stromal cells into spinal cord: through cerebrospinal fluid

Koji Nishida, Nobuhiro Tanaka, Kazuyoshi Nakanishi, Naosuke Kamei, Takahiko Hamasaki, Shinobu Yanada, Yu Mochizuki and Mitsuo Ochi

Department of Orthopaedic Surgery, Graduate School of Biomedical Sciences, Hiroshima University, Hiroshima, Japan

Correspondence and requests for reprints to Dr Koji Nishida, MD, Department of Orthopaedic Surgery, Graduate School of Biomedical Sciences, Hiroshima University, 1-2-3 Kasumi, Minami-ku, Hiroshima 734-8551, Japan
Tel: +81 82 257 5233; fax: +81 82 257 5234; e-mail: kl2nish@aol.com

Sponsorship: This study was supported in part by grants-in-aid to M.O. from the Japan Ministry of Education, Culture, Sports, Science and Technology (No. 16209045).

Received 8 May 2006; accepted 16 May 2006

We established a new magnetic targeting system in which bone marrow stromal cells migrate through the cerebrospinal fluid to the desired site in the spinal cord in rats. Subarachnoid injection has been reported as a minimally invasive method of transplantation of bone marrow stromal cells for spinal cord injury. It may be, however, less effective than direct injection into the spinal cord in terms of cell delivery. After implantation of a magnet, subarachnoid injection of bone marrow stromal cells labeled with magnetic beads was performed. Greater numbers of bone marrow stromal cells aggregated on the surface of the spinal cord owing to the magnetic force. This targeting system may be a useful tool in minimally invasive transplantation of bone marrow stromal cells for the treatment of spinal cord injury. *NeuroReport* 17:1269–1272

Keywords: bone marrow stromal cells, cerebrospinal fluid, spinal cord, targeting, transplantation

Introduction

Bone marrow stromal cells (BMSCs) are pluripotent stem cells that can be easily harvested, cultured and used in autologous transplantation. They have the potential of differentiating into muscle, cartilage, bone and adipose tissue. They also act as support cells by producing an array of trophic factors and cytokines [1].

Transplantation of BMSCs has been reported to promote regeneration of the spinal cord after spinal cord injury in animal studies [2–4]. In previous studies, cell transplantation was performed by direct injection of BMSCs into the spinal cord with a needle. Local injection into an injured spinal cord may, however, be clinically harmful. In addition, Bakshi *et al.* [5] pointed out that this method would require major neurosurgery, and would not allow suitable delivery of multiple therapeutic doses.

Transplantation through the cerebrospinal fluid (CSF) has been evaluated as a minimally invasive method [4–6]. The lumbar puncture technique is safe and can be performed repeatedly in clinical situations. However, when cells are injected into the CSF, they quickly become diluted and must travel a long distance from the lumbar entry point to the injury lesion. Subarachnoid injection may be less effective than direct injection in terms of cell delivery. Inoue *et al.* [7] compared the effect of direct injection or intravenous injection of various concentrations of bone marrow cells to a demyelinated lesion in the spinal cord, and reported that intravenous administration of a larger number of cells was required to attain the same relative density of remyelination achieved by direct injection. Subarachnoid injection of a larger number of cells may be required to attain the same outcome as direct injection. The number of BMSCs is, however, limited in clinical treatment. The authors considered it is necessary to develop a cell delivery system through the CSF.

We previously demonstrated magnetic targeting systems with magnetic liposome or labeled cells. Delivery of bone morphogenic protein-2 to bone [8], transforming growth factor-β1 to cartilage [9], anticancer agents to a tumor [10,11] and natural killer cells to a tumor [12] resulted in desirable accumulation at the target lesion. Arbab *et al.* [13] also successfully performed magnetic targeting of BMSCs into the liver.

The present study is the first trial to examine whether BMSCs can be targeted to a particular site in the spinal cord. BMSCs were labeled with Feridex, which is composed of super paramagnetic iron oxide nanoparticles and is commercially available as a magnetic resonance imaging contrast agent approved by the United States Food and Drug Administration.

The purpose of this study was to establish a magnetic targeting system for effective and minimally invasive transplantation of BMSCs through the CSF to the desired site in the spinal cord.

Materials and methods

Our research methods were reviewed and approved by the ethical committee of the Hiroshima University.

Bone marrow stromal cells culture

BMSCs were obtained from the tibias of 12-week-old, male, green fluorescent protein (GFP)-expressing transgenic Sprague–Dawley rats. The marrow suspension was seeded in Dulbecco's modified Eagle's medium-high glucose (Gibco, Grand Island, New York, USA) containing 10% heat-inactivated fetal bovine serum (Sigma, St Louis, Missouri, USA) on 100-mm dishes and cultured at 37°C in a humidified atmosphere of 95% air and 5% CO_2 [14]. When the proliferating colonies had nearly reached confluence, the adherent cells were harvested with 0.25% trypsin–ethylene diaminetetraacetic acid. After three or four passages, we used the cells for transplantation.

Labeling of bone marrow stromal cells with Feridex

BMSCs were labeled for 24 h with 25 μg Fe/ml Feridex (11.2 mg Fe/ml; Takeda, Osaka, Japan) and 375 ng/ml PLL (Sigma). Briefly, Feridex and PLL were added to a culture medium and incubated at room temperature for 60 min. This medium was added to the BMSCs culture as described previously [15]. After trypsinization, 1×10^5 cells were suspended in 50 μl of phosphate-buffered saline (PBS) as the injection solution for each rat.

Rats for transplantation via lumbar puncture

A total of 10 Sprague–Dawley rats (weighing 330–360 g) were used as the recipients. After anesthesia with pentobarbital sodium (40 mg/kg, intraperitoneally), T7 laminectomy was carried out microscopically. A neodymium magnet (380 mT, 5 mm in diameter, 3 mm in height) was placed in the para-vertebral muscles at the T7 level of rats in the magnet group (n=5), whereas a nonmagnetic metal (same material, same size) was placed in a similar manner in the rats in the nonmagnet group (n=5). At the L4–5 intervertebral space, the dura was exposed with partial removal of the L5 spinous process and L4–5 ligamentum flavum [6]. Fifty microliters of PBS solution containing 1×10^5 BMSCs were injected into the subarachnoid space with a 29-G needle. Each layer of muscle and skin was sutured tightly. After transplantation, rats were kept on a 30° slope in the head-down position for 30 min.

Tissue harvest and evaluation

One day after transplantation, the rat was perfused with PBS and 4% paraformaldehyde intracardially under deep anesthesia. The spinal cord was dissected, postfixed overnight in 4% paraformaldehyde and transferred to 10 and 20% sucrose solutions. The spinal cord was cut into a 10-mm-long block whose center was at the T7 level. After freezing, it was cut into longitudinal sagittal sections in a cryostat at 20 μm thickness. Under a fluorescence microscope (Leica Microsystems, Wetzler, Germany), the areas of aggregations of GFP-positive cells on each 10-mm-long section were calculated and added using the Scion Image for Windows image analysis program (Scion Corporation, Frederick, Maryland, USA). Results were expressed as mean ± standard deviation (n=5 in each group). To investigate the effect of the magnetic force, the area of the aggregations of GFP-positive cells in the magnet group was compared with that in the nonmagnet group by the Mann–Whitney test. One spinal cord in the magnet group was cut into longitudinal sections at 5 μm thickness, and stained with Prussian Blue stain.

Results

Macroscopic findings

The spinal cords were collected and observed macroscopically before making frozen sections. Brown spots exist on the spinal cord at the T7 level in all five rats in the magnet group (Fig. 1a), whereas there were no brown spots on the spinal cords of the rats in the nonmagnet group (Fig. 1b). BMSCs labeled with magnetic beads were concentrated at the T7 level of the spinal cord of rats in the magnet group as observed by microscopic examination of the brown spots, but not in the rats in the nonmagnet group.

Microscopic findings

Upon fluorescence microscopy of the sagittal slices, aggregations of GFP-positive cells were observed mainly on the dorsal surface of the spinal cords of rats in the magnet group (Fig. 2a). There were, however, few aggregations of GFP-positive cells in the nonmagnet group (Fig. 2b). In the magnet group, the GFP-positive cells had not infiltrated into the parenchyma but were located on the surface of the spinal cord (Fig. 3a). Most of the cell aggregations were stained by Prussian Blue stain (Fig. 3b). These findings indicated that the cell clusters were composed of transplanted cells labeled with magnetic beads.

Comparison between the magnet and nonmagnet groups

The area of GFP-positive clusters on serial sections of the spinal cord was measured. The mean area in the magnet group (n=5) was 229 498 ± 71 390 μm^2 and that in the nonmagnet group (n=5) was 7745 ± 3118 μm^2, showing a significant difference (P < 0.01).

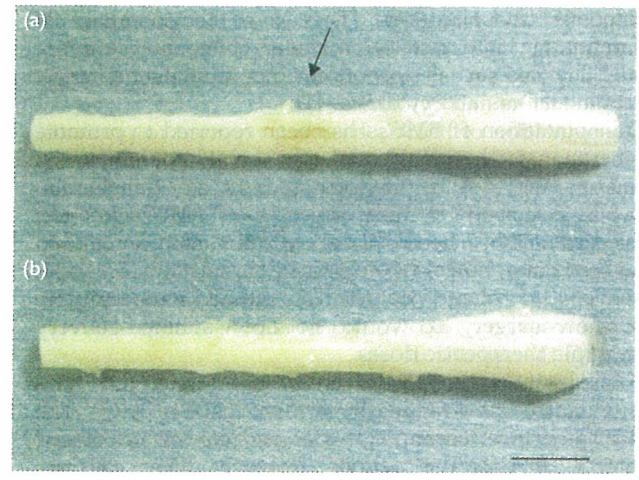

Fig. 1 Spinal cords that were resected 1 day after transplantation of bone marrow stromal cells (BMSCs) in the dorsal view (the center of the resected spinal cord is the T7 level, left: rostral). A magnet or nonmagnet metal had been placed in the para-vertebral muscles at the T7 level, and BMSCs labeled with magnetic beads were injected at the L4–5 intervertebral space. Brown-colored areas (arrow) exist in the magnet group (a), whereas there were no brown-colored areas in the nonmagnet group (b). Bar=5 mm.

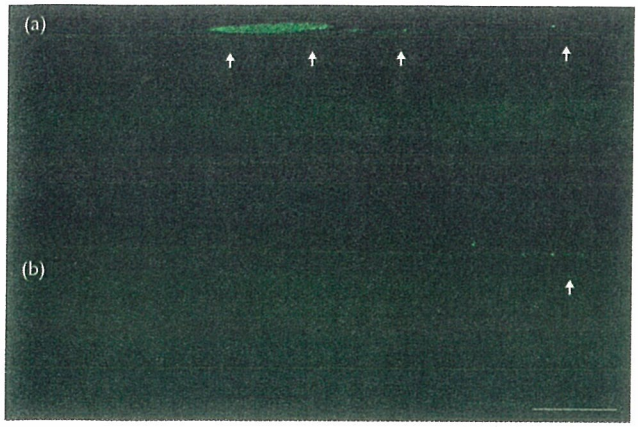

Fig. 2 Fluorescence microscopy of sagittal slices of the spinal cord (left: rostral, up: dorsal). Aggregations of green fluorescent protein (GFP)-positive cells (arrow) exist on the dorsal side of the spinal cord in the magnet group (a), whereas there were few GFP-positive cells on the spinal cord in the nonmagnet group (b). Bar=1 mm.

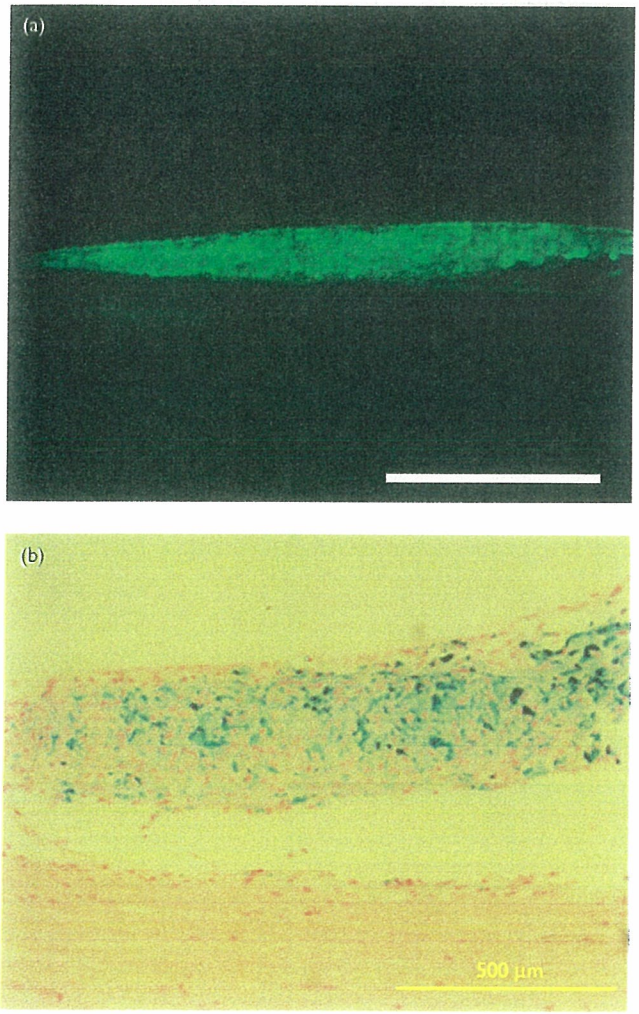

Fig. 3 Cell aggregations on the dorsal side of the spinal cord of rats in the magnet group. Green fluorescent protein-positive cells were mainly observed on the dorsal cord, and they did not infiltrate the spinal cord parenchyma, as viewed under a fluorescence microscope (a). The majority of cells in the aggregations were stained by Prussian Blue (b) (left: rostral, up: dorsal). Bar=500 μm.

Discussion

In the present study, we demonstrated that BMSCs transplanted via lumbar puncture could migrate through the CSF and aggregate at the T7 level of the spinal cord using the magnetic targeting system. Macroscopic examination of the spinal cords revealed brown spots on the dorsal spinal cord at the T7 level in rats in the magnet group (Fig. 1a), and the majority of cells in the cell aggregations were stained by Prussian Blue stain (Fig. 3b). These findings show that the magnetic force effectively gathered cells labeled with magnetic beads.

If BMSCs are injected into the CSF in the absence of a targeting system, the cells would quickly become diluted. As the number of BMSCs that can be collected and the period of culture are limited in clinical treatment, the number of BMSCs available for autologous transplantation tends to be small. Therefore, aggregation of BMSCs at the injured lesion is beneficial.

We previously used BMSCs for tissue engineering in animals [14,16,17] and for clinical treatment [18]. In the present study, we used BMSCs for transplantation to the spinal cord. BMSCs, embryonic stem cells, neural progenitor cells and other cell types could have been labeled with magnetic beads [13,15,17,19–21]. Several cell sources can also be used in the magnetic targeting. In addition, if magnetic liposome complex is used in our system, cytokines or neurotrophic factors can be delivered. Multiple dosages of cells and cytokines can be injected through the CSF, and delivered to the lesion with the present system.

We established a cell delivery system with a permanent magnet as an internal magnetic force in this study. We have already succeeded in magnetic targeting by an external magnetic force to the legs [11] or knee joints [16]. A magnetic targeting system through the CSF by an external magnetic force is promising for the clinical treatment of spinal cord injury.

To the best of our knowledge, there has been no report on magnetic targeting of cells into the spinal cord. We demonstrated a new cell delivery system through the CSF. Our magnetic cell targeting system is a useful tool for efficient and minimally invasive transplantation to injuries or diseases of the spinal cord. Further studies are needed to determine the therapeutic effect of these cells.

Conclusion

The present study successfully demonstrated minimally invasive transplantation of BMSCs via lumbar puncture, followed by magnetic targeting of BMSCs through the CSF to the desired site in the spinal cord.

References

1. Chopp M, Li Y. The treatment of neural injury with marrow stromal cell. *Lancet Neurol* 2002; 1:92–100.
2. Chopp M, Zhang XH, Li Y, Wang L, Chen J, Lu D, *et al*. Spinal cord injury in rat: treatment with bone marrow stromal cell transplantation. *NeuroReport* 2000; 11:3001–3005.
3. Hofstetter CP, Schwarz EJ, Hess D, Widenfalk J, Manira AE, Prockop DJ, *et al*. Marrow stromal cells form guiding strands in the injured spinal cord and promote recovery. *Proc Natl Acad Sci USA* 2002; 99:2199–2204.
4. Ohta M, Suzuki Y, Noda T, Ejiri Y, Dezawa M, Ktataoka K, *et al*. Bone marrow stromal cells infused into the cerebrospinal fluid promote functional recovery of the injured rat spinal cord with reduced cavity formation. *Exp Neurol* 2004; 187:266–278.

5. Bakshi A, Hunter C, Swanger S, Leopore A, Fischer I. Minimally invasive delivery of stem cells for spinal cord injury: advantages of the lumbar puncture technique. *J Neurosurg* 2004; **3**:330–337.
6. Satake K, Lou J, Lenke LG. Migration of mesenchymal stem cells through cerebrospinal fluid into injured spinal cord tissue. *Spine* 2004; **18**:1971–1979.
7. Inoue M, Honmou O, Oka S, Houkin K, Hashi K, Kocsis JD. Comparative analysis of remyelinating potential of focal and intravenous administration of autologous bone marrow cells into the rat demyelinated spinal cord. *Glia* 2003; **44**:111–118.
8. Matsuo T, Sugita T, Kubo T, Yasunaga Y, Ochi M, Murakami T. Injectable magnetic liposomes as a novel carrier of recombinant human BMP-2 for bone formation in a rat bone-defect model. *J Biomed Mater Res A* 2003; **66**:747–754.
9. Tanaka H, Sugita T, Yasunaga Y, Shimose S, Deie M, Kubo T, *et al.* Efficiency of magnetic liposomal transforming growth factor-beta 1 in the repair of articular cartilage defects in a rabbit model. *J Biomed Mater Res A* 2005; **73**:255–263.
10. Kubo T, Sugita T, Shimose S, Nitta Y, Ikuta Y, Murakami T. Targeted delivery of anticancer drugs with intravenously administered magnetic liposomes in osteosarcoma-bearing hamsters. *Int J Oncol* 2000; **17**:309–315.
11. Nobuto H, Sugita T, Kubo T, Shimose S, Yasunaga Y, Murakami T, *et al.* Evaluation of systemic chemotherapy with magnetic liposomal doxorubicin and a dipole external electromagnet. *Int J Cancer* 2004; **109**:627–635.
12. Nakashima Y, Deie M, Yanada S, Sharman P, Ochi M. Magnetically labeled human natural killer cells, accumulated in vitro by an external magnetic force, are effective against HOS osteosarcoma cells. *Int J Oncol* 2005; **27**:965–971.
13. Arbab AS, Jordan EK, Wilson LB, Yocum GT, Lewis BK, Frank JA. *In vivo* trafficking and targeted delivery of magnetically labeled stem cells. *Hum Gene Ther* 2004; **15**:351–360.
14. Ito Y, Tanaka N, Fujimoto Y, Yasunaga Y, Ishida O, Ochi M. Bone formation using novel interconnected porous calcium hydroxyapatite ceramic hybridized with cultured marrow stromal stem cells derived from Green rat. *J Biomed Mater Res A* 2004; **69**:454–461.
15. Kostura L, Kraitchman DL, Mackay AM, Pittenger MF, Bulte JW. Feridex labeling of mesenchymal stem cells inhibits chondrogenesis but not adipogenesis or osteogenesis. *NMR Biomed* 2004; **17**:513–517.
16. Ochi M, Adachi N, Nobuto H, Yanada S, Ito Y, Agung M. Articular cartilage repair using tissue engineering technique: novel approach with minimally invasive procedure. *Artif Organs* 2004; **28**:28–32.
17. Yanada S, Ochi M, Adachi N, Nobuto H, Agung M, Kawamata S. Effects of CD44 antibody- or RGDS peptide-immobilized magnetic beads on cell proliferation and chondrogenesis of mesenchymal stem cells. *J Biomed Mater Res A* 2006; **77**:773–784.
18. Adachi N, Ochi M, Deie M. Transplant of mesenchymal stem cells and hydroxyapatite ceramics to treat severe osteochondral damage after septic arthritis of the knee. *J Rheumatol* 2005; **32**:1615–1618.
19. Jendelova P, Herynek V, Urdzikova L, Glogarova K, Kroupova J, Andersson B, *et al.* Magnetic resonance tracking of transplanted bone marrow and embryonic stem cells labeled by iron oxide nanoparticles in rat brain and spinal cord. *J Neurosci Res* 2004; **76**:232–243.
20. Bulte JW, Douglas T, Witwer B, Zhang SC, Strable E, Lewis BK, *et al.* Magnetodendrimers allow endosomal magnetic labeling and *in vivo* tracking of stem cells. *Nat Biotechnol* 2001; **19**:1141–1147.
21. Hamasaki T, Tanaka N, Ishida O, Yanada S, Kamei N, Fujiwara Y, *et al.* Characterization of labeled neural progenitor cells for magnetic targeting. *NeuroReport* 2005; **16**:1641–1645.

Delayed Gadolinium-enhanced MR to Determine Glycosaminoglycan Concentration in Reparative Cartilage after Autologous Chondrocyte Implantation: Preliminary Results[1]

Atsuya Watanabe, MD
Yuichi Wada, MD
Takayuki Obata, MD
Takuya Ueda, MD
Mitsuru Tamura, PE
Hiroo Ikehira, MD
Hideshige Moriya, MD

Purpose: To prospectively evaluate delayed gadolinium-enhanced magnetic resonance (MR) imaging of cartilage for assessment of glycosaminoglycan (GAG) concentration in reparative cartilage after autologous chondrocyte implantation (ACI).

Materials and Methods: The study was approved by the ethics review committee of the National Institute of Radiological Sciences, and informed consent was obtained from all patients. The study group comprised nine knees of nine patients (six male, three female; mean age at ACI, 21.2 years ± 7.5 [standard deviation]; age range, 13–35 years) who had undergone ACI and second-look arthroscopy with biopsy. MR imaging was performed at 1.5 T before and after intravenous injection of anionic gadopentetate dimeglumine. The precontrast R1 ($R1_{pre}$), postcontrast R1 ($R1_{post}$), and difference between $R1_{pre}$ and $R1_{post}$ ($\Delta R1$) were measured in reparative cartilage and normal cartilage. GAG concentrations in cartilage biopsy specimens were measured by using high-performance liquid chromatography. To evaluate delayed gadolinium-enhanced MR imaging of cartilage for assessment of GAG concentration, the authors defined the relative $R1_{pre}$, relative $R1_{post}$, and relative $\Delta R1$ (ie, $R1_{pre}$, $R1_{post}$, or $\Delta R1$, respectively, in reparative cartilage divided by that in normal cartilage) and the relative GAG concentration (ie, GAG concentration in reparative cartilage divided by that in normal cartilage). They then examined the relationships between relative $R1_{pre}$, relative $R1_{post}$, relative $\Delta R1$, and relative GAG by using correlation analysis.

Results: A significant correlation between relative $\Delta R1$ and relative GAG concentration ($r = 0.818$, $P < .05$) was observed. However, no significant correlation between relative $R1_{pre}$ and relative GAG concentration ($r = 0.010$, $P = .983$) or between relative $R1_{post}$ and relative GAG concentration ($r = 0.660$, $P = .106$) was observed.

Conclusion: Study results indicate that pre- and postcontrast imaging is necessary for delayed gadolinium-enhanced MR imaging evaluation of reparative cartilage after ACI.

[1] From the Departments of Orthopaedic Surgery (A.W., Y.W., H.M.) and Radiology (T.U.), Graduate School of Medicine, Chiba University, Chiba, Japan; and Department of Medical Imaging, National Institute of Radiological Sciences, 4-9-1 Anagawa, Inage-Ku, Chiba-Shi, Chiba 263-8555, Japan (A.W., T.O., M.T., H.I.). Received February 5, 2005; revision requested April 4; revision received May 2; final version accepted June 3. Supported by Health Science Research grants from the Ministry of Health and Welfare of Japan and by grants-in-aid from the Ministry of Education, Culture, Sports, Science and Technology. **Address correspondence to** T.O. (e-mail: *t_obata@nirs.go.jp*).

Articular cartilage is a type of hyaline cartilage characterized by an extracellular matrix that contains a fine network of collagen and abundant proteoglycan that is tolerant to dynamic load. However, articular cartilage, which lacks blood vessels and has low cell density, is known to have limited healing potential (1,2). Thus, the development of a full-thickness articular cartilage defect, especially in weight-bearing areas, can cause severe pain and joint dysfunction, which may eventually develop into osteoarthritis (3,4). Attempts to repair articular cartilage defects have involved the use of various marrow-stimulation techniques, including subchondral drilling (5,6), abrasion chondroplasty (7,8), and microfracture (9,10). The goal of these techniques is to recruit pluripotent mesenchymal cells from the bone marrow to synthesize new fibrocartilage that will cover the defect (11,12). However, fibrocartilage repair tissue tends to have weak mechanical strength and is prone to degeneration over time, which leads to the return of the clinically important symptoms (13).

Autologous chondrocyte implantation (ACI) was introduced by Brittberg et al (14) in 1994 as a treatment for full-thickness defects of the articular cartilage in the knee. Repairing a hyaline cartilage defect by using ACI could improve the long-term durability of the reparative cartilage and prevent the onset of late osteoarthritis. Various groups in clinical follow-up studies have reported good to excellent results (15,16). However, several authors who have conducted histologic examinations and/or biochemical analyses of ACI repair sites have reported that the reparative cartilage was not always identical to the hyaline cartilage found in normal cartilage tissue (17–19). In some patients, the tissue filling the defect was identified as fibrocartilage or a mixture of fibrocartilage and hyaline cartilage—tissues that, compared with pure hyaline cartilage, have a lower proteoglycan concentration and a less-organized collagen network, which can lead to early deterioration after ACI. Until recently, quantitative evaluation of reparative cartilage could be achieved only by using invasive methods such as second-look arthroscopy with biopsy.

Magnetic resonance (MR) imaging has the potential to enable the determination of tissue composition, and several MR imaging techniques for monitoring the structure of articular cartilage have been developed and evaluated (20,21). An MR technique called delayed gadolinium-enhanced MR imaging of cartilage has been developed as a sensitive and specific method of measuring the concentration of glycosaminoglycan (GAG), a component of articular cartilage that is critical to its mechanical strength (22–25). The biochemical basis of delayed gadolinium-enhanced MR imaging of cartilage is as follows: Because GAG is composed of abundant carboxyl and sulfate groups, it is negatively charged within the cartilage matrix. Anionic gadopentetate dimeglumine (Magnevist; Schering, Berlin, Germany), given a sufficient time after its injection to penetrate the cartilage, will distribute inversely to the concentration of negatively charged cartilaginous GAG. Thus, as a noninvasive method of indirectly monitoring the GAG concentration in cartilage, delayed gadolinium-enhanced MR imaging is potentially a useful method of assessing the extent to which reparative cartilage is composed of articular cartilage, which is tolerant of mechanical stress.

In published clinical studies (26) to evaluate the effectiveness of gadolinium-enhanced MR imaging for measuring cartilage degeneration, the concentration of anionic gadopentetate dimeglumine has been estimated by using measurements of the R1 (in 1/sec) after intravenous contrast material injection (ie, postcontrast R1 [$R1_{post}$]) only, because differences in the R1 before contrast material injection (ie, precontrast R1 [$R1_{pre}$]) between degenerated and normal cartilage were so slight that the influence of $R1_{pre}$ was thought to be negligible. However, it remains unknown whether the influence of $R1_{pre}$ is negligible also in the evaluation of reparative cartilage after ACI, especially since the histologic appearance of reparative cartilage may be considerably different from that of normal cartilage. Thus, the aim of our study was to prospectively evaluate delayed gadolinium-enhanced MR imaging of cartilage for assessment of the GAG concentration in reparative cartilage after ACI.

Materials and Methods

Patients

The study group comprised nine knees (two right knees, seven left knees) of nine patients (six male, three female) who had undergone ACI and second-look arthroscopy with biopsy. At the time of ACI, the patients' mean age was 21.2 years ± 7.5 (standard deviation) (age range, 13–35 years) and their mean defect size was 4.6 cm^2 ± 2.2 (range, 2.3–10.5 cm^2). The implantation sites were seven medial femoral condyles and two lateral femoral condyles. Six patients had osteochondritis dissecans, and three had a trauma-induced osteochondral defect. The study was approved by the ethics review committee of the National Institute of Radiological Sciences, and informed consent was obtained from all patients.

Chondrocyte Implantation Surgery

The ACI procedure described by Brittberg et al (14) was performed. Briefly, cartilage was removed from a non-

Published online before print
10.1148/radiol.2383050173

Radiology 2006; 239:201–208

Abbreviations:
ACI = autologous chondrocyte implantation
GAG = glycosaminoglycan
ΔR1 = difference between $R1_{pre}$ and $R1_{post}$
$R1_{post}$ = postcontrast R1
$R1_{pre}$ = precontrast R1

Author contributions:
Guarantors of integrity of entire study, A.W., T.O.; study concepts/study design or data acquisition or data analysis/interpretation, all authors; manuscript drafting or manuscript revision for important intellectual content, all authors; manuscript final version approval, all authors; literature research, all authors; clinical studies, all authors; statistical analysis, all authors; and manuscript editing, all authors

Authors stated no financial relationship to disclose.

weight-bearing area of the affected knee during the initial arthroscopy. Chondrocytes were then isolated from the cartilage and cultured for approximately 4 weeks in a laboratory (Genzyme Tissue Repair, Cambridge, Mass). The cultured chondrocytes were injected into the defect covered with a periosteal flap. The patients began active movements of the knee without weight bearing immediately after surgery. Weight bearing was resumed at postoperative week 6 and increased to full activity during the next 4 weeks.

MR Imaging

MR imaging was performed a mean of 22.7 months ± 11.0 (standard deviation) (range, 13–38 months) after the ACI by using a 1.5-T MR system (Gyroscan Intera; Philips Medical Systems, Best, the Netherlands) with a quadrature knee coil. All patients were examined before and 2 hours after an intravenous injection of anionic gadopentetate dimeglumine by using the same MR imaging protocol on both occasions. For the precontrast MR imaging examination, two authors (A.W. and T.O., with 7 and 16 years of experience in knee MR imaging, respectively) identified the section that depicted the center of the reparative cartilage on a set of routine T1-weighted sagittal images. The T1-weighted imaging parameters were as follows: 500/17 (repetition time msec/echo time msec), a 150 × 150-mm field of view, a 3.0-mm section thickness, a 512 × 512 matrix, two signals acquired, a 52.6-kHz bandwidth, and a fast spin-echo factor of six.

Three authors (A.W., T.O., M.T.) performed quantitative R1 measurements on the selected section by using the inversion-recovery method with a single-section acquisition. Inversion-recovery fast spin-echo MR images were obtained by using inversion times of 50, 100, 200, 400, 800, and 1600 msec. The inversion-recovery imaging parameters were as follows: 1800/28, a 130 × 130-mm field of view, a 3.0-mm section thickness, a 512 × 512 matrix, two signals acquired, a 64.1-kHz bandwidth, and a fast spin-echo factor of six. The total imaging time required to acquire the series of inversion-recovery MR images was about 17 minutes. At MR imaging, the local concentration of anionic gadopentetate dimeglumine in the tissue ($Gd\text{-}DTPA^{2-}$) is determined by using the following equation:

$$Gd\text{-}DTPA^{2-} = (1/r) \cdot (R1_{post} - R1_{pre}), \quad (1)$$

where r is the relaxivity of anionic gadopentetate dimeglumine in the tissue (in $mmol/L^{-1} \cdot sec^{-1}$) and R1 equals 1 divided by the longitudinal relaxation time.

During postcontrast MR imaging, a set of routine sagittal T1-weighted images was acquired by using the precontrast T1-weighted imaging parameters described earlier. The postcontrast T1-weighted images were compared with the precontrast T1-weighted images to identify the postcontrast section that corresponded to the precontrast section previously determined to depict the center of the reparative cartilage. If none of the postcontrast sections corresponded closely enough to the precontrast section showing the center of the reparative cartilage, the patient's knee position was adjusted and a new set of routine sagittal T1-weighted images was acquired. Quantitative R1 measurements were then performed on this selected section by using the inversion times and imaging parameters described earlier.

We followed the postcontrast MR imaging protocol reported on by Burstein et al (26). Anionic gadopentetate dimeglumine, at a dose of 0.2 mmol per kilogram of body weight, was intravenously injected in a single bolus. Immediately after the injection, the patient exercised the knee by walking up and down stairs for 10 minutes. Postcontrast MR imaging was performed 2 hours after administration of the contrast agent. The exercise and delay after the injection were necessary to allow the contrast agent to penetrate the cartilage.

Image Analysis

For all nine knees, maps of the cartilage constructed by using $R1_{pre}$ and $R1_{post}$ values were generated from the six precontrast and six postcontrast inversion-recovery MR images, respectively, by using commercially available software (Dr. View; Asahikasei, Tokyo, Japan) with a specialized three-parameter exponential curve fit module. We used a registration technique to correct for patient motion between each inversion-recovery MR imaging examination with the Dr. View software. With use of MATLAB software (The Mathworks, Natick, Mass), a color-coded R1-constructed map of the cartilage, with the cartilage area segmented manually, was overlaid on the inversion-recovery image obtained by using the longest inversion time. On the color scale, blue represented areas of low R1 and red represented areas of high R1.

Measurements of $R1_{pre}$, $R1_{post}$, and the difference between $R1_{pre}$ and $R1_{post}$ ($\Delta R1$) in both reparative cartilage and normal cartilage were obtained in all patients. For these measurements, the region of interest was drawn over the entire area of the reparative cartilage, with all hypertrophic periosteal tissue excluded. The region of interest in the normal cartilage was drawn over a weight-bearing area of the femoral condyle from the surface to the basal area, and the size of this region was drawn as large as the size of the reparative cartilage (200–300 pixels). To avoid including damaged cartilage, the region of interest in the normal cartilage was drawn approximately 2 cm from the reparative cartilage. To standardize the procedure, all regions of interest were drawn by a single investigator (A.W., with 7 years of experience in knee MR imaging).

Histologic and Biochemical Analyses and Arthroscopy

Two authors (Y.W. and A.W., with 22 and 8 years of experience in arthroscopy, respectively) performed second-look arthroscopy with biopsy a mean of 12.4 months ± 0.5 (range, 12–13 months) after ACI. The mean interval between biopsy and MR imaging was 13.2 months ± 8.4 (range, 1–26 months). Biopsy specimens were taken from all nine reparative cartilage sites and from seven normal cartilage sites by